

UCSF

UC San Francisco Electronic Theses and Dissertations

Title

Neuronal mechanisms regulating oligodendrocyte precursor cell differentiation and axon selection for myelination

Permalink

<https://escholarship.org/uc/item/3pp4x3bk>

Author

Osso, Lindsay Alexandra

Publication Date

2021

Peer reviewed|Thesis/dissertation

Neuronal mechanisms regulating oligodendrocyte precursor cell differentiation and axon selection for myelination


by
Lindsay Alexandra Osso

DISSERTATION
Submitted in partial satisfaction of the requirements for degree of
DOCTOR OF PHILOSOPHY

in
Neuroscience

in the
GRADUATE DIVISION
of the
UNIVERSITY OF CALIFORNIA, SAN FRANCISCO

Approved:


DocuSigned by:

05586C7D64D24A2... Samuel Pleasure
Chair

DocuSigned by:

Jonah Chan

DocuSigned by:

Jennifer L Whistler

DocuSigned by:

9A805C3F0428410... Eric J Huang

Committee Members

To the women before me who made this possible

ACKNOWLEDGEMENTS

First, I am exceedingly grateful to the UCSF Neuroscience Graduate Program for providing me with the opportunity to work at the leading edge of science and for fostering an open and collegial community of scientists. I extend my gratitude to the students and faculty who donate their time to keep this program running and always improving, and to our program administrators, Pat Veitch and Lucita Nacionales, for their grounding presence and guidance in navigating the bureaucracy.

I am forever indebted to Jonah Chan for welcoming me into his lab. I would like to thank him for the career mentorship and opportunities, and for his scientific mentorship and council. Jonah's trust in me has been an empowering gift. I hope to honor his philosophy of thinking big and creatively and not being afraid to challenge dogma.

I would like to thank the many past and present Chan lab members, Ainhoa Etxeberria, Kae-Jiun Chang, Kelsey Rankin, Maggie Yeung, Monique Lillis, Sarah Raissi, Sonia Mayoral, Stephanie Redmond, Wendy Xin, and Yun-An Shen, for their support, advice, mentorship, and friendship over the years. They have made me into the scientist I am today and I will miss working with them dearly.

I want to thank the members of my thesis committee, Sam Pleasure, Jennifer Whistler, and Eric Huang, for their encouragement, perspective, and support.

I am so grateful for my San Francisco friends for making this new country feel like a home and for so thoroughly enriching my time here, and for all my friends for their interest, support, and love through the ups and downs of graduate school.

I am indebted to Justin Berot-Burns for the sacrifices he has made for me to be able to follow my dreams and for making every day better than it could have possibly been without him.

I want to thank my parents, Martin and Rietta Osso, for everything they did to get me to where I am today and for their unwavering support of my decision to move 4,500 km from home. They have also been the ultimate role models of lifelong learning.

I would like to acknowledge the important role that my previous research supervisors, Phil Barker and Jack Antel, played in my scientific career. The research opportunities they gave me during my undergraduate days were critical for my admission to UCSF. And the fact that they were paid opportunities meant I could take them.

Finally, I would like to acknowledge the mice who died in the service of discovery, without whom none of this would have been possible.

CONTRIBUTIONS

Chapter 1 is reproduced from:

Osso, L.A., and Chan, J.R. (2017). Architecting the myelin landscape. *Curr. Opin. Neurobiol.* 47, 1–7.

L.A.O. wrote the manuscript with feedback from J.R.C. and all members of the Chan laboratory.

Chapter 2 is currently under peer review. Lindsay A. Osso and Jonah R. Chan conceived of and designed all experiments. Kelsey A. Rankin contributed to tissue processing, immunostaining, and imaging for **Figure 2.5**, **Figure 2.6**, **Figure 2.7**, and **Figure 2.8**. L.A.O. performed and analyzed all other experiments. L.A.O. wrote the manuscript with feedback from J.R.C. and all members of the Chan laboratory.

Chapter 3 was written by Lindsay A. Osso.

Neuronal mechanisms regulating oligodendrocyte precursor cell differentiation and axon selection for myelination

Lindsay A. Osso

ABSTRACT

Myelin is the insulating membrane concentrically wrapped around some axons, which serves to increase the speed and efficiency of action potential propagation. In the central nervous system (CNS), myelin is formed by oligodendrocytes, which differentiate from self-renewing oligodendrocyte precursor cells (OPCs) throughout life. While factors intrinsic to oligodendrocyte lineage cells control certain features of myelination, extrinsic cues also play an important role in regulating myelination both in development and in response to experience. Thus far, identifying these extrinsic molecular players has proved challenging. **Chapter 1** of this dissertation describes the known patterns of CNS myelination and provides a framework to understand how neuronal signaling could influence this architecture, using it to evaluate previous work in this field. **Chapter 2** presents our experimental work identifying one of these extrinsic neuronal cues for myelination as the neuropeptide dynorphin. We demonstrate that dynorphin, which is released from neurons upon high levels of activity, promotes experience-dependent myelination. Following forced swim stress, an experience that induces striatal dynorphin release, we observe increased striatal OPC differentiation and myelination, which is abolished by deleting dynorphin or blocking its endogenous receptor, kappa opioid receptor (KOR). We find dynorphin also promotes developmental OPC differentiation and myelination, and demonstrate that this effect requires KOR expression specifically on

OPCs. We characterize dynorphin-expressing neurons and use genetic sparse-labeling to trace their axonal projections. Surprisingly, we find they are unmyelinated normally and following forced swim stress, in part due to their small size. We propose a new model whereby experience-dependent and developmental myelination is mediated by unmyelinated, neuropeptide-expressing neurons that promote OPC differentiation for the myelination of neighboring axons. **Chapter 3** evaluates our findings in the context of the framework presented in **Chapter 1** and comments on the significance of our work.

TABLE OF CONTENTS

CHAPTER 1: Architecting the myelin landscape	1
1.1 Summary.....	1
1.2 The myelin landscape	1
1.3 The intrinsic nature of oligodendrocyte myelination	3
1.4 Extrinsic factors regulating oligodendrocyte axon selection	5
1.5 A role for axons in oligodendrocyte myelination	9
1.6 Axonal cues for axon selection	10
1.7 Wrapping it up.....	15
CHAPTER 2: Experience-dependent myelination following stress is mediated by the neuropeptide dynorphin	17
2.1 Summary.....	17
2.2 Introduction	17
2.3 Results	21
2.4 Discussion.....	42
2.5 Materials and methods.....	49
CHAPTER 3: Conclusion	63
3.1 Synthesis	63
3.2 Significance.....	67
3.3 Reflections	68
REFERENCES	70

LIST OF FIGURES

CHAPTER 1: Architecting the myelin landscape

Figure 1.1: Different mechanisms of axon selection could produce the same CNS myelination patterns 6

CHAPTER 2: Experience-dependent myelination following stress is mediated by the neuropeptide dynorphin

Figure 2.1: *Cspg4-CreERTM*; *Mapt-mGFP* mice allow for identification of newly differentiated oligodendrocytes 22

Figure 2.2: Forced swim stress promotes striatal OPC differentiation and myelination 23

Figure 2.3: Blocking dynorphin-KOR signaling prevents stress-induced OPC differentiation and myelination 25

Figure 2.4: Dynorphin knock-out mice have deficits in developmental OPC differentiation and myelination redundant with the loss of OPC KORs 28

Figure 2.5: Identification of several neuronal subtypes expressing dynorphin 31

Figure 2.6: Dynorphin is not expressed in glia 32

Figure 2.7: Upper cortical layer II/III dynorphin-expressing cells rarely colocalize with interneuron markers 33

Figure 2.8: Deeper cortical layer dynorphin-expressing cells rarely colocalize with non-Martinotti cell markers 34

Figure 2.9: Axons of dynorphin-expressing neurons are unmyelinated normally and following forced swim stress 36

Figure 2.10: Axons of dynorphin-expressing neurons in the corpus callosum are unmyelinated..... 38

Figure 2.11: Dynorphin-expressing neurons have small diameter axons 40

Figure 2.12: Model of dynorphin-induced OPC differentiation and subsequent myelination of axons of non-dynorphin expressing neurons..... 43

LIST OF TABLES

CHAPTER 2: Experience-dependent myelination following stress is mediated by the neuropeptide dynorphin

Table 2.1: Key resources 51

Table 2.2: Genotyping primers and amplified fragment sizes 54

CHAPTER 3: Conclusion

Table 3.1: Factors regulating oligodendrocyte formation or axon selection..... 63

CHAPTER 1: Architecting the myelin landscape

1.1 Summary

Myelin increases the speed and efficiency of action potential propagation. Yet, not all axons are myelinated and some axons are discontinuously myelinated, prompting the question of how myelinating glia select axons for myelination. Whereas myelination by Schwann cells depends on axonal induction, oligodendrocytes can form myelin membrane in the absence of axons. However, oligodendrocytes alone cannot architect the complex myelination patterns of the central nervous system (CNS) and recent advances have implicated axonal signaling in this process. This review considers how oligodendrocytes and their precursors could be influenced by *inductive*, *attractive*, *permissive*, *repulsive*, and *preventative* cues, and discusses recent evidence identifying synaptic activity and membrane-bound adhesion molecules as such cues directing axon selection.

1.2 The myelin landscape

Myelin, the insulating membrane concentrically wrapped around axons, accelerates impulse propagation and offloads neuronal energy expenditure. Despite these advantages, not all axons are myelinated and some axons are only intermittently myelinated. In the peripheral nervous system (PNS), Schwann cells myelinate solely large diameter axons (Voyvodic, 1989), with individual Schwann cells each myelinating only one axon segment. By contrast, CNS myelination patterns are more complicated. During development, myelination proceeds in a stereotyped sequence with different

regions being myelinated at different times as oligodendrocyte precursor cells (OPCs), which are distributed throughout the CNS, differentiate into myelinating oligodendrocytes (Foran and Peterson, 1992; Kinney et al., 1988). OPC differentiation and myelination continues into adulthood, albeit at a much slower rate (Hughes et al., 2013; Yeung et al., 2014; Young et al., 2013). Unlike Schwann cells, each oligodendrocyte extends many processes to myelinate several different axon segments. The smallest caliber CNS axons are never myelinated but there is significant overlap in the diameters of myelinated and unmyelinated axons (Sturrock, 1980), whereas other CNS structures geometrically similar to axons – dendrites, blood vessels, and glial processes – remain unmyelinated, with rare exceptions.

Recent volumetric reconstructions of cortical tissue have further refined our understanding of CNS myelination. Intriguingly, myelination may depend on neuronal subtype: a recent study found that parvalbumin-positive basket cells are essentially the only type of GABAergic interneuron with myelinated axons in the adult mouse neocortex (Micheva et al., 2016). Another study contested the prevailing dogma of myelination as an all-or-none phenomenon; rather, many pyramidal axons in the adult mouse neocortex are intermittently myelinated, with large unmyelinated gaps between myelinated sections (Tomassy et al., 2014), a configuration distinct from nodes of Ranvier that separate individual myelin sheaths (internodes) to permit saltatory conduction.

This partial myelin coverage likely reflects the need to balance the advantages of myelination with overall energy (Harris and Attwell, 2012) and space constraints, and likely contributes to the precise control of circuit timing (Hoz and Simons, 2015), underscoring the importance of appropriate myelin localization. In the case of intermittent

myelination along a single axon, unmyelinated gaps could provide space for new myelin formation to fine-tune myelination patterns as circuit activity changes in the adult. This review will focus on our current understanding of how these intricate patterns of myelination are established.

1.3 The intrinsic nature of oligodendrocyte myelination

Given that sensory and motor axons that pass between the CNS and PNS are myelinated by both oligodendrocytes and Schwann cells, it seems intuitive that CNS and PNS axons would use similar mechanisms to control myelin formation. In the PNS, axons play a necessary and *inductive* role in their own myelination. Neuregulin-1 type III is required for Schwann cell maturation and myelination of PNS axons (Taveggia et al., 2005) and its expression level determines myelin sheath thickness (Michailov et al., 2004). Importantly, its ectopic suprathreshold expression *induces* the myelination of normally unmyelinated axons (Taveggia et al., 2005), demonstrating its importance in determining myelination fate.

However, neuregulin-1 type III is largely dispensable for CNS myelination (Brinkmann et al., 2008; Taveggia et al., 2008). In fact, several aspects of oligodendrocyte myelination proceed successfully without molecular axonal signaling altogether. Cultured OPCs intrinsically differentiate into oligodendrocytes, which, remarkably, can form compact myelin around inert polystyrene fibers (Lee et al., 2012). In fact, certain properties of *in vivo* myelination can be explained by how oligodendrocyte lineage cells intrinsically interact with axonal geometries. Neither OPCs or oligodendrocytes will ensheath or wrap synthetic fibers with a diameter smaller than 0.3 μ m, a similar threshold

to that observed *in vivo* (Lee et al., 2012), indicating that oligodendrocyte lineage cells directly sense fiber geometries. Geometric sensing by oligodendrocyte lineage cells may also explain the general correlation between internode length and axon diameter *in vivo* (Ibrahim et al., 1995; Murray and Blakemore, 1980) as this correlation persists with synthetic fibers (Bechler et al., 2015). Exactly how oligodendrocyte lineage cells detect radial axon size remains elusive, but they may utilize properties such as curvature or circumference to do so. Curvature-inducing components could impose a physical limit on oligodendrocyte lineage cell membrane curvature that prevents wrapping of highly curved, subthreshold diameter axons. Alternatively, oligodendrocyte lineage cells could sense their own membrane curvature as they wrap (for an example of curvature sensing at a similar scale, see Bridges et al., 2016) and avoid wrapping axons above a threshold curvature. Another approach could be for oligodendrocyte lineage cells to infer axonal circumference by sensing the length of one wrap of their membrane around an axon (for a potential mechanism of length sensing, see Rishal et al., 2012). Upon completing one wrap, an oligodendrocyte lineage cell process would contact itself. If the process length was subthreshold, the process would retract upon self-contact, preventing wrapping. Retraction of a growing OPC process upon contact with another process of the same OPC has been observed in the adult mouse cortex (Hughes et al., 2013); the same mechanism could operate in this context as well. To avoid retraction upon self-contact, the oligodendrocyte lineage process would have to exceed a threshold length. At this threshold, the length sensing machinery would initiate a rapid downregulation of the self-repulsion mechanism locally within the wrapping process (e.g. by internalizing cell adhesion molecules), enabling self-contact and myelination of suprathreshold

circumference axons. Similar mechanisms could also be used to correlate internode length with radial axon size.

Regional differences in oligodendrocyte lineage cells, which likely emerge after OPC specification (Kessaris et al., 2006), may explain some differences in myelination between CNS regions. OPCs isolated from developing spinal cord form longer internodes upon differentiation than do those isolated from neocortex in cultures with synthetic fibers or neurons (Bechler et al., 2015), reproducing the differences in internode length observed between these regions *in vivo* (Chong et al., 2012). Another study demonstrated that the higher levels of differentiation and myelination in white matter (Dawson et al., 2003) might be partially explained by differences between white matter and gray matter OPCs. Adult white matter OPCs transplanted into either adult white matter or gray matter differentiated more efficiently than adult gray matter OPCs transplanted into either region (Viganò et al., 2013).

1.4 Extrinsic factors regulating oligodendrocyte axon selection

Whereas intrinsic properties of oligodendrocyte lineage cells might be helpful for setting up some basic features of the myelin landscape, they cannot independently produce the complex and specific myelination patterns observed in the CNS. For example, the relationship between myelin sheath thickness and axon diameter (Bishop et al., 1971) is not reproduced with synthetic fibers (Bechler et al., 2015), and the ratio of internode length to axon diameter is actually highly variable *in vivo* (Ford et al., 2015; Ibrahim et al., 1995; Murray and Blakemore, 1980). In particular, since oligodendrocytes are not programmed to myelinate a specific type of axon (Almeida et al., 2011; Fanarraga et al.,

1998; Osanai et al., 2017) and many suprathreshold diameter axons are not myelinated *in vivo* (Sturrock, 1980), other factors must contribute to the regulation of axon selection. Indeed, extrinsic factors have an important role in this process. For myelination of the appropriate axons at the appropriate time, oligodendrocytes must be present and they must know where to form myelin – two components that can be influenced by extrinsic factors. By influencing virtually every aspect of oligodendrocyte development, extrinsic signals can affect the distribution of oligodendrocytes at any time. Furthermore, extrinsic signals can influence where individual oligodendrocytes localize their myelin sheaths.

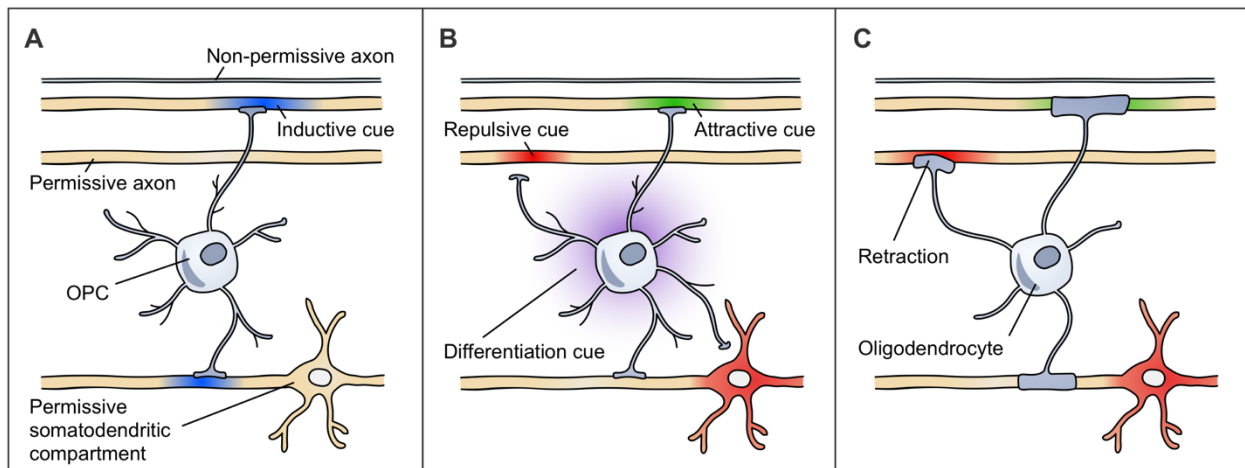


Figure 1.1: Different mechanisms of axon selection could produce the same CNS myelination patterns. These three models are non-exhaustive and not mutually-exclusive. Structures with suprathreshold diameters are shown in yellow as permissive. The first axon has a subthreshold diameter, rendering it non-permissive. **(A)** An inductive cue (blue) turns on in axons to initiate their myelination. Shown here, an OPC senses a threshold myelination need from the second and fourth axons that causes the OPC to differentiate and myelinate these axons. These axons are among the permissive structures. **(B)** OPCs respond to attractive (green), permissive (yellow), and repulsive (red) cues on axons and other cellular compartments that regulate the contacts that OPCs make and the eventual placement of myelin sheaths. The OPC processes retract from repulsive cues on the third axon and the somatodendritic compartment. Upon differentiation, this cell will myelinate the second and fourth axons. The differentiation cue (purple) is uncoupled from axon selection. **(C)** Oligodendrocytes respond to attractive (green), permissive (yellow), and repulsive (red) cues that affect sheath initiation or stability. Retraction of an early sheath in response to a repulsive cue on the third axon is shown. This oligodendrocyte myelinates the second and fourth axons.

Axons, as the substrates for myelination, are logical candidates for being the source of these extrinsic cues. Axons might precisely regulate the timing of their myelination by expressing dynamic cues. An *inductive* cue could turn on, or a converse *preventative* cue could turn off, in an axon to initiate its myelination. OPCs, which actively survey their environment (Hughes et al., 2013; Kirby et al., 2006) and receive synaptic inputs from axons (Maldonado and Angulo, 2015), are well-positioned to integrate such cues from multiple axons. A threshold level of change in these axons could cause OPCs to differentiate and to myelinate these axons. By utilizing a combined differentiation/axon selection cue (**Figure 1.1 A**), this system would be extremely efficient in matching the number of oligodendrocytes and their internodes to the axons requiring myelination at any time.

Alternatively, differentiation and axon selection could be uncoupled (**Figure 1.1 B, C**) (Almeida and Lyons, 2016). Differentiation could occur either through an actively regulated mechanism or through one that is indiscriminately applied wherein oligodendrocytes that differentiated in excess of available axons would eventually die (Barres et al., 1992; Calver et al., 1998; Trapp et al., 1997). Axon selection could be performed by either OPCs (**Figure 1.1 B**) or oligodendrocytes (**Figure 1.1 C**). OPCs could identify axons to myelinate upon their eventual differentiation (**Figure 1.1 B**), or, once differentiated, oligodendrocytes could become receptive to axonal cues that regulate either sheath initiation or stability (**Figure 1.1 C**). The axon selection cues described below could apply to either cell type. *Inductive* or *preventative* axon selection cues could operate in this context (although they are not illustrated in **Figure 1.1 B, C**). In the case of unregulated OPC differentiation, both the patterns and timing of myelination would be

controlled solely by the axons that become available for myelination based on their changing expressions of *inductive* or *preventative* cues. In the case of actively regulated OPC differentiation, the timing of *inductive* (or *preventative*) cue onset (or offset) would have to precisely coordinate with the timing of the regulated differentiation mechanism to be able to initiate myelination of an axon during the seemingly short period between OPC differentiation and the termination of new sheath formation (Czopka et al., 2013; Hughes et al., 2013) (although, see Yeung et al., 2014). With regulated OPC differentiation, it would instead be simpler for oligodendrocyte lineage cells to respond to axon selection cues that are not dynamically regulated, perhaps having existed on axons long before differentiation occurs. Such cues would influence myelin localization but not its timing. These cues could be termed *attractive* or *repulsive*, positively or negatively biasing an axon's selection for myelination by either altering the distribution or number of oligodendrocyte internodes (**Figure 1.1 B, C**).

Finally, regardless of whether differentiation and axon selection are coupled or not, axons must be *permissive* for myelination – a feature that permits their myelination but does not guarantee it (e.g. suprathreshold axon diameters). Axon *permissiveness* may be static or dynamically regulated (e.g. as subthreshold axons grow). An outstanding question in the field is whether structures that are simply *permissive* – lacking any *inductive* or *attractive* cues – are myelinated in the CNS (as illustrated in **Figure 1.1 B, C**). While the models of axon selection presented here are not mutually exclusive, their conceptual separation is useful for establishing a framework to evaluate research in this field.

1.5 A role for axons in oligodendrocyte myelination

Efforts to elucidate the role of CNS axons in their own myelination have greatly benefited from innovations in sparse (low-efficiency recombination), targeted genetic manipulations and live imaging with single-cell resolution. A creative genetic approach generating zebrafish with supernumerary large caliber spinal cord Mauthner axons provided compelling evidence for the influence of axons on an individual oligodendrocyte's myelination patterns. These extra axons caused Mauthner axon-associated oligodendrocytes to extend more internodes to myelinate more Mauthner axons than normal, and even prompted non-Mauthner axon-associated oligodendrocytes to myelinate Mauthner axons. Notably, oligodendrocyte numbers did not change (Almeida et al., 2011), supporting a model wherein axonal cues alter axon selection independent of OPC differentiation (**Figure 1.1 B, C**).

A recent study in mice demonstrated that axonal cues can have a considerably broader impact on oligodendrocyte development and myelination. Knocking-out *Pten* specifically from cerebellar granule cells, which increased axon caliber to suprathreshold diameters and altered gene expression, caused ectopic proliferation and differentiation of OPCs and myelination of granule cell axons in the normally unmyelinated cerebellar molecular layer (Goebbels et al., 2017). It is unclear whether all of these effects are mediated through the same or disparate mechanisms – or exactly what those mechanisms are. Could these effects be entirely attributable to increasing axon caliber to a *permissive* level, or are molecular changes also involved? Intriguingly, ectopic myelination was still observed when *Pten* was only sparsely knocked-out (Goebbels et al., 2017). Identifying whether the axons lacking PTEN were the ones that were

myelinated in this sparse manipulation will provide important information on the spatial nature of this change. Moving forward, this genetic model could be a tractable system to investigate the mechanisms by which axons regulate their own myelination.

1.6 Axonal cues for axon selection

An axon selection cue must be sufficiently localized to facilitate the distinction between axons as well as geometrically similar substrates in close proximity. Membrane-bound cues or those released at synapses both meet this requirement.

Synaptic activity

OPCs receive glutamatergic and GABAergic synaptic inputs from axons and express a myriad of other neurotransmitter receptors (Larson et al., 2016; Maldonado and Angulo, 2015), perhaps to inform OPCs of a myelination need. A model often termed “activity-dependent myelination” posits that changes in synaptic inputs to OPCs could serve as an *inductive* cue, causing OPC differentiation and myelination of the axons providing modified inputs, perhaps even converting axon-OPC synapses into a myelinating sheath (**Figure 1.1 A**) (Almeida and Lyons, 2014). This process could shape brain development based on experience or contribute to learning by modifying circuit timing.

Two landmark *in vivo* studies energized this hypothesis. Optogenetic stimulation of neurons in the mouse premotor cortex increased proliferation and differentiation of OPCs (Gibson et al., 2014), which presumably generate new myelin. Similarly, training mice to run on a complex wheel increases OPC proliferation and differentiation in the corpus callosum. In fact, generating new OLs, and presumably new myelin, was required

for mice to properly learn the task (McKenzie et al., 2014). Since simply increasing OPC density can enhance differentiation (Rosenberg et al., 2008), the direct effects of neuronal activity on OPC differentiation in these studies is unclear. A follow-up study using the same motor learning paradigm showed that differentiation occurs from the existing pool of OPCs (Xiao et al., 2016), suggesting that subsequent OPC proliferation may occur in response to local OPC differentiation, as was observed in live imaging of cortical OPC dynamics (Hughes et al., 2013). An important next step is to analyze where new myelin is localized in these paradigms; are axons with increased activity *inducing* their own myelination by expressing a combined differentiation/axon selection cue (**Figure 1.1 A**) or might axonal activity simply act as a differentiation cue without affecting axon selection (**Figure 1.1 B**)?

A recent study supports the latter. Social isolation of adult mice reduced OPC differentiation, the number of myelinated axons, and myelin thickness in the prefrontal cortex (PFC) and caused social withdrawal, all of which were rescued by oral administration of the pro-differentiation compound clemastine (Liu et al., 2016). If the presumably reduced activity of specific sociability-related axons during social isolation prevented these axons from expressing an *inductive* cue that would normally cause OPC differentiation and their selection for myelination (**Figure 1.1 A**), it's unlikely that the ostensibly indiscriminate upregulation of OPC differentiation by clemastine would rescue these deficits. More plausibly, PFC activity from social interaction upregulates overall OPC differentiation without affecting axon selection, and is important for providing sufficient numbers of oligodendrocytes to myelinate the relevant axons, which utilize other cues to regulate their selection for myelination (**Figure 1.1 B, C**).

Notably, other studies have found no (Makinodan et al., 2012) or opposite (Etxeberria et al., 2016) effects of neuronal activity on OPC differentiation, while others have observed differences in properties such as oligodendrocyte internode number (Makinodan et al., 2012; Mensch et al., 2015), length (Etxeberria et al., 2016; Hines et al., 2015; Koudelka et al., 2016), or thickness (Gibson et al., 2014; Liu et al., 2012, 2016; Makinodan et al., 2012). Of these, two pioneering studies found a direct role for the synaptic activity of individual axons in regulating their selection for myelination. Treatment of zebrafish with tetrodotoxin (TTX) to block action potentials reduced the myelination of *phox2b*⁺ axons in the spinal cord without affecting total internode or oligodendrocyte numbers, suggesting that these axons use neuronal activity to facilitate their myelination (Hines et al., 2015). Indeed, expressing tetanus toxin (TeNT), which prevents synaptobrevin/VAMP2-mediated synaptic exocytosis, in individual *phox2b*⁺ axons substantially reduced the myelination of these axons (Hines et al., 2015). The same was true for TeNT expression in single reticulospinal axons (Mensch et al., 2015). TeNT expression globally or specifically in neurons caused individual oligodendrocytes to form 30% fewer internodes (Hines et al., 2015; Mensch et al., 2015).

The results with TTX versus TeNT suggest different mechanisms of activity-mediated axon selection, highlighting the importance of elucidating the specific mechanisms involved to resolve the sources of these discrepancies. The TTX data support a model of competition between axons for myelination. When neuronal activity was abolished, *phox2b*⁺ axons lost their competitive advantage, and so other axons were myelinated in their place. Conversely, the TeNT data suggests that the axon selection cue used by these axons promotes their myelination by increasing the number of

internodes per oligodendrocyte, perhaps by affecting downstream oligodendrocyte Fyn kinase signaling (Czopka et al., 2013). One study observed increased sheath retractions in the TeNT condition by live imaging (Hines et al., 2015) – a possible explanation for the decreased sheath number per oligodendrocyte in this condition. Despite the reduction in excitatory synaptic input as OPCs differentiate into early oligodendrocytes, these cells continue to respond to glutamate (Biase et al., 2010; Kukley et al., 2010) and maintain some glutamate receptor expression (Marques et al., 2016; Zhang et al., 2014). The increase in sheath retractions in response to blocking synaptic exocytosis along with the observation that synaptic vesicles preferentially stopped at nascent ensheathment sites (Hines et al., 2015) imply that early myelinating oligodendrocytes do respond to synaptic inputs and that these inputs are important for axon selection (**Figure 1.1 C**).

Could synaptic activity-mediated axon selection account for CNS myelination patterns? Different neuronal subtypes utilize different neurotransmitters and have distinct firing rates, features oligodendrocyte lineage cells could use to identify specific axonal subtypes to myelinate (Micheva et al., 2016). But since these features do not differ within a single neuron, how could synaptic activity produce intermittent myelination along a single axon (Tomassy et al., 2014)? Axons could synapse with OPCs unevenly along their lengths. Alternatively, cues from an individual axon could remain consistent but the surrounding environment could affect that axon's competitiveness for myelination.

Membrane-bound adhesion molecules

Not surprisingly, not all axons utilize synaptic activity to regulate their selection for myelination. While individual reticulospinal neurons expressing TeNT had reduced myelin

coverage, TeNT expression in individual commissural primary ascending axons had no effect on their myelination (Koudelka et al., 2016). What other cues might axons use to regulate their selection for myelination?

Adhesion molecules, which mediate cell-cell interactions, are logical candidates. In fact, several axonal adhesion molecules negatively regulate OPC differentiation and/or myelination, and seem to downregulate their expression as myelination proceeds (e.g. Jagged1 (Wang et al., 1998), PSA-NCAM (Charles et al., 2000), or Lsamp (Sharma et al., 2015)). It is tempting to regard these molecules as potential *preventative* cues for myelination, wherein their removal from an axon would initiate myelination of that axon, potentially in conjunction with causing OPC differentiation. Future studies genetically manipulating these molecules sparsely in axons will elucidate their potential roles in axon selection.

Recently, the adhesion molecule JAM2 was identified as a negative regulator of myelination with no effect on OPC differentiation. It is expressed by the somatodendritic compartment of cultured spinal cord neurons and prevents myelination of this cellular compartment. Oligodendrocytes ectopically myelinate the somata and dendrites of cultured *Jam2* knock-out spinal cord neurons, and increased ectopic myelination of PAX2+ neuronal somata was found in the dorsal spinal cord of *Jam2* knock-out mice (Redmond et al., 2016). This study confirms the presence of *repulsive* cues that shape where OLs form internodes. It also suggests either that neuronal somata express sufficiently *attractive* cues such that they become myelinated when inhibition is reduced, or that simply *permissive* structures can be myelinated in the CNS (**Figure 1.1 B, C**). Intriguingly, JAM2-Fc coated micropillars are *repulsive* to both cultured OPCs and OPC-

derived oligodendrocytes (Redmond et al., 2016), indicating that OPCs respond to substrate selection cues that influence their eventual internode placement, independent of that cue's ability to affect differentiation (**Figure 1.1 B**). Likewise, contact-mediated self-repulsion by OPCs (Hughes et al., 2013; Kirby et al., 2006) supports the idea that these cells are well-equipped with adhesion molecules to regulate the placement of their processes.

Could similar *repulsive* cues exist that prevent the myelination of glia or blood vessels? Might there be adhesion molecules, *attractive* or *repulsive*, that distribute unevenly along axons or differentially between different neuronal subtypes, shaping CNS myelination patterns (Micheva et al., 2016; Tomassy et al., 2014)?

1.7 Wrapping it up

The question of how axons are selected for myelination has been historically difficult to answer. However, new research efforts utilizing sparse genetic manipulations and high-resolution live imaging have begun to shed light on this complex issue and will be essential moving forward. Despite *in vitro* work establishing the intrinsic nature of oligodendrocyte myelination, current research has clearly demonstrated that axons have a role in their selection for myelination. The extent of their contribution and the molecular players remain to be determined and will be fruitful grounds for future studies.

This review has focused primarily on the mechanisms through which axons might communicate with oligodendrocyte lineage cells to regulate their initial myelin coverage. While myelin sheath retractions have been observed in early oligodendrocytes, it is not yet clear how ongoing communication between axons and oligodendrocytes might alter

myelin coverage in the long term. In addition to affecting axon selection, evidence suggests that axons can regulate internode length and sheath thickness, properties that – like axon selection – affect conduction velocity and energy usage. It remains a beautiful mystery as to how these properties are regulated in concert with one another, and to what extent axons are active players in this coordination, functioning as grand architects of the ever-changing myelin landscape.

CHAPTER 2: Experience-dependent myelination following stress is mediated by the neuropeptide dynorphin

2.1 Summary

Emerging evidence implicates experience-dependent myelination in learning and memory. However, the specific signals underlying this process remain unresolved. We demonstrate that the neuropeptide dynorphin, which is released from neurons upon high levels of activity, promotes experience-dependent myelination. Following forced swim stress, an experience that induces striatal dynorphin release, we observe increased striatal oligodendrocyte precursor cell (OPC) differentiation and myelination, which is abolished by deleting dynorphin or blocking its endogenous receptor, kappa opioid receptor (KOR). We find dynorphin also promotes developmental OPC differentiation and myelination, and demonstrate that this effect requires KOR expression specifically on OPCs. We characterize dynorphin-expressing neurons and use genetic sparse-labeling to trace their axonal projections. Surprisingly, we find they are unmyelinated normally and following forced swim stress, in part due to their small size. We propose a new model whereby experience-dependent and developmental myelination is mediated by unmyelinated, neuropeptide-expressing neurons that promote OPC differentiation for the myelination of neighboring axons.

2.2 Introduction

Brain plasticity in response to experience is considered essential for learning and memory. Historically, experience-dependent plasticity has been understood to involve

changes in synaptic strength (Takeuchi et al., 2014) and structure (Fu and Zuo, 2011), but recent studies have found that non-neuronal cells also respond to experience and can, in turn, regulate neuronal function and behavior (Cheadle et al., 2020; Lacoste et al., 2014; Murphy-Royal et al., 2020; Whiteus et al., 2014; Xin and Chan, 2020).

In particular, the oligodendrocyte lineage can be profoundly impacted by experience (Xin and Chan, 2020). Oligodendrocytes form myelin, the concentrically wrapped membrane that insulates axons and facilitates rapid and efficient action potential conduction. Each oligodendrocyte extends numerous processes to form myelin internodes around many different axons. Oligodendrocytes arise from self-renewing OPCs, which populate the entire central nervous system (CNS) and undergo a burst of differentiation and subsequent myelination in development, followed by ongoing – but slowing – OPC differentiation and myelination throughout life (Hill et al., 2018; Hughes et al., 2018; Sturrock, 1980; Wang et al., 2020). This results in the myelination of the axons of some neuronal subtypes while others remain unmyelinated or partially myelinated into adulthood (Micheva et al., 2016; Sturrock, 1980; Tomassy et al., 2014). Recent studies have shown that the experiences of motor, spatial, and contextual learning (Bacmeister et al., 2020; McKenzie et al., 2014; Pan et al., 2020; Steadman et al., 2020; Xiao et al., 2016), socialization (Swire et al., 2019), and sensory stimulation (Hughes et al., 2018) can promote OPC differentiation and myelination. This process, termed experience-dependent myelination, seems to play an important role in learning and memory (McKenzie et al., 2014; Pan et al., 2020; Steadman et al., 2020; Wang et al., 2020; Xiao et al., 2016). Other studies have found that oligodendrocyte lineage cells can be similarly impacted by neuronal activity (Gibson et al., 2014; Mitew et al., 2018), leading to the

hypothesis that experience acts on the oligodendrocyte lineage through increases in neuronal activity, likely involving activity-dependent neuronal vesicular release.

To advance our understanding of experience-dependent myelination and the role it plays in brain function and plasticity, there is a clear need to determine precisely which molecular signals regulate this process. However, to date, no signal has been shown to underlie experience-dependent myelination. We sought to address this question in the context of forced swim stress, an experience involving well-defined signaling pathways and brain regions. We found that forced swim stress induced a pronounced increase in OPC differentiation and myelination in the striatum. Next, we interrogated the mechanisms regulating this novel form of experience-dependent myelination. Acute stress signaling involves several hormones and neuropeptides, including the neuropeptide family of dynorphin, which contributes to the development or expression of depressive, anxious, and addictive behaviors following acute stress (Knoll and Carlezon, 2010). The dynorphin family of peptides derive from prodynorphin, encoded by *Pdyn* (Schwarzer, 2009). These peptides are stored in large dense-core vesicles (Drake et al., 1994; Yakovleva et al., 2006) and are released from neurons following high levels of neuronal activity (Simmons et al., 1995; Terman et al., 1994; Yakovleva et al., 2006). Crucially, dynorphin is released in the striatum following forced swim stress (Bruchas et al., 2008; Schindler et al., 2012).

Previously, we performed an unbiased screen for small molecules that promote OPC differentiation. We identified a cluster of molecules that activate the endogenous dynorphin receptor, kappa opioid receptor (KOR), on OPCs to dramatically increase the rate of OPC differentiation into myelinating oligodendrocytes (Mei et al., 2016). Mice

lacking KOR on OPCs have deficits in OPC differentiation and myelination in development as well as following a demyelinating lysolecithin lesion in the adult corpus callosum (Mei et al., 2016). These results suggest that the endogenous KOR ligand, dynorphin, might play an important role in OPC differentiation and myelination. Taken together, these features of dynorphin – its striatal release following forced swim stress and its agonism for KOR – led us to investigate its potential role as a novel signal underlying experience-dependent myelination. By genetically or pharmacologically blocking dynorphin-KOR signaling, we abolished striatal stress-induced OPC differentiation, indicating that dynorphin is essential for this novel form of experience-dependent myelination.

Furthermore, we found that dynorphin also promotes developmental OPC differentiation and myelination and demonstrated that this requires the expression of KORs specifically on OPCs. To determine the source of dynorphin, we characterized dynorphin-expressing cells and identified several neuronal subtypes. In light of previous work showing that the activity of some neurons both promotes OPC differentiation as well as their own selection for myelination (Mitew et al., 2018) and the untested possibility that these two processes could be regulated by the same signal, we investigated whether dynorphin also acts as a signal to promote the selection of dynorphin-expressing neurons for myelination. Using genetic sparse-labeling to trace the axonal projections of dynorphin-expressing neurons, we, surprisingly, found that they were overwhelmingly unmyelinated both under normal conditions and following forced swim stress, in part due to their small size. Collectively, these results identify dynorphin as a novel signal

underlying experience-dependent and developmental myelination, whose release from unmyelinated neurons promotes OPC differentiation for the myelination of other axons.

2.3 Results

Forced swim stress promotes striatal OPC differentiation in adult mice

Several recent studies have found that experience can promote OPC differentiation and myelination (Bacmeister et al., 2020; Hughes et al., 2018; McKenzie et al., 2014; Pan et al., 2020; Steadman et al., 2020; Swire et al., 2019; Xiao et al., 2016), but the molecular signals mediating this process remain unresolved. We first sought to determine whether acute stress would promote experience-dependent myelination, using the classic paradigm of forced swim stress. Mice were subjected to a 15 min swim on the first day, followed by four 6 min swim sessions 24 h later, while littermate controls remained in their home cage (**Figure 2.2 A**).

To assess new OPC differentiation in adult mice, we took advantage of a genetic method that allows for the visualization of newly formed oligodendrocytes with membrane-GFP (mGFP) (Mitew et al., 2018; Wang et al., 2020; Young et al., 2013). We crossed *Cspg4*-CreERTM mice to *Mapt*-mGFP reporter mice to generate *Cspg4*-CreERTM; *Mapt*-mGFP mice. *Cspg4* (NG2) is expressed in OPCs, allowing for tamoxifen-dependent recombination in OPCs, while the *Mapt*-mGFP reporter is expressed in oligodendrocytes, preventing mGFP expression until differentiation. Thus, following tamoxifen administration, OPCs that undergo recombination and differentiate can be visualized as mGFP-expressing oligodendrocytes (**Figure 2.1 A-D** and **Figure 2.2 D, G**). Following forced swim stress, we observed a 1.8-fold increase in the density of mGFP+MBP+

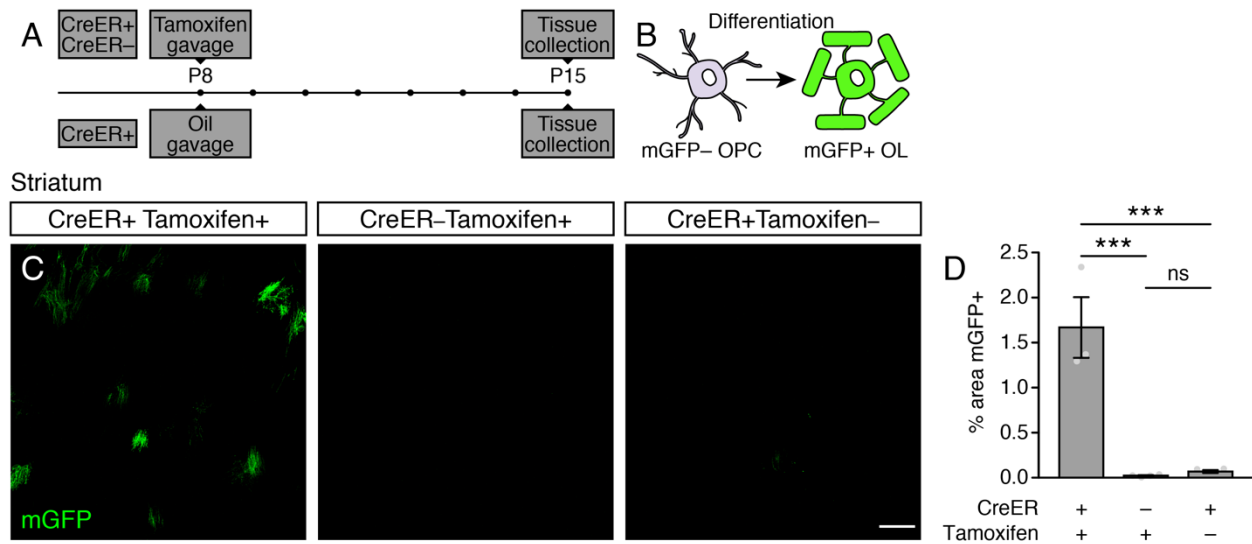


Figure 2.1: *Cspg4*-CreERTM; *Mapt*-mGFP mice allow for identification of newly differentiated oligodendrocytes. (A) Experimental paradigm for tamoxifen or oil administration and tissue collection performed in *Cspg4*-CreERTM; *Mapt*-mGFP and *Mapt*-mGFP littermates at postnatal day (P) 8, when a high rate of developmental OPC differentiation readily allows for visualization of newly differentiated mGFP+ oligodendrocytes in CreER+ mice gavaged with tamoxifen. (B) Recombined OPCs express mGFP upon differentiation. Abbreviation: OL = oligodendrocyte. (C) Representative images of mGFP+ oligodendrocytes in CreER+ mice gavaged with tamoxifen, CreER- mice gavaged with tamoxifen, or CreER+ mice gavaged with oil. (D) Quantification of percentage of area that is mGFP+ in each condition (CreER+Tamoxifen+: 1.668 ± 0.3364, n = 3; CreER-Tamoxifen+: 0.02229 ± 0.006689, n = 4; CreER+Tamoxifen-: 0.06861 ± 0.01689, n = 4; ANOVA, P = 0.0001, F(2,8) = 33.68; Tukey's, CreER+Tamoxifen+ vs. CreER-Tamoxifen+, P = 0.0002, q(8) = 10.43; CreER+Tamoxifen+ vs. CreER+Tamoxifen-, P = 0.0002, q(8) = 10.14; CreER-Tamoxifen+ vs. CreER+Tamoxifen-, P = 0.9728, q(8) = 0.3171). Scale bar, 100 μm. Data are presented as mean ± s.e.m.; significance determined using one-way ANOVA and Tukey's multiple comparisons; ***P < 0.001; ns = not significant.

myelinating oligodendrocytes in the striatum (Figure 2.2 B, C). By contrast, we observed no change in OPC differentiation in the cortex (Figure 2.2 E, F), indicating that forced swim stress induces regionally specific increases in OPC differentiation. These results demonstrate that acute stress can promote striatal OPC differentiation and myelination in a novel form of experience-dependent myelination.

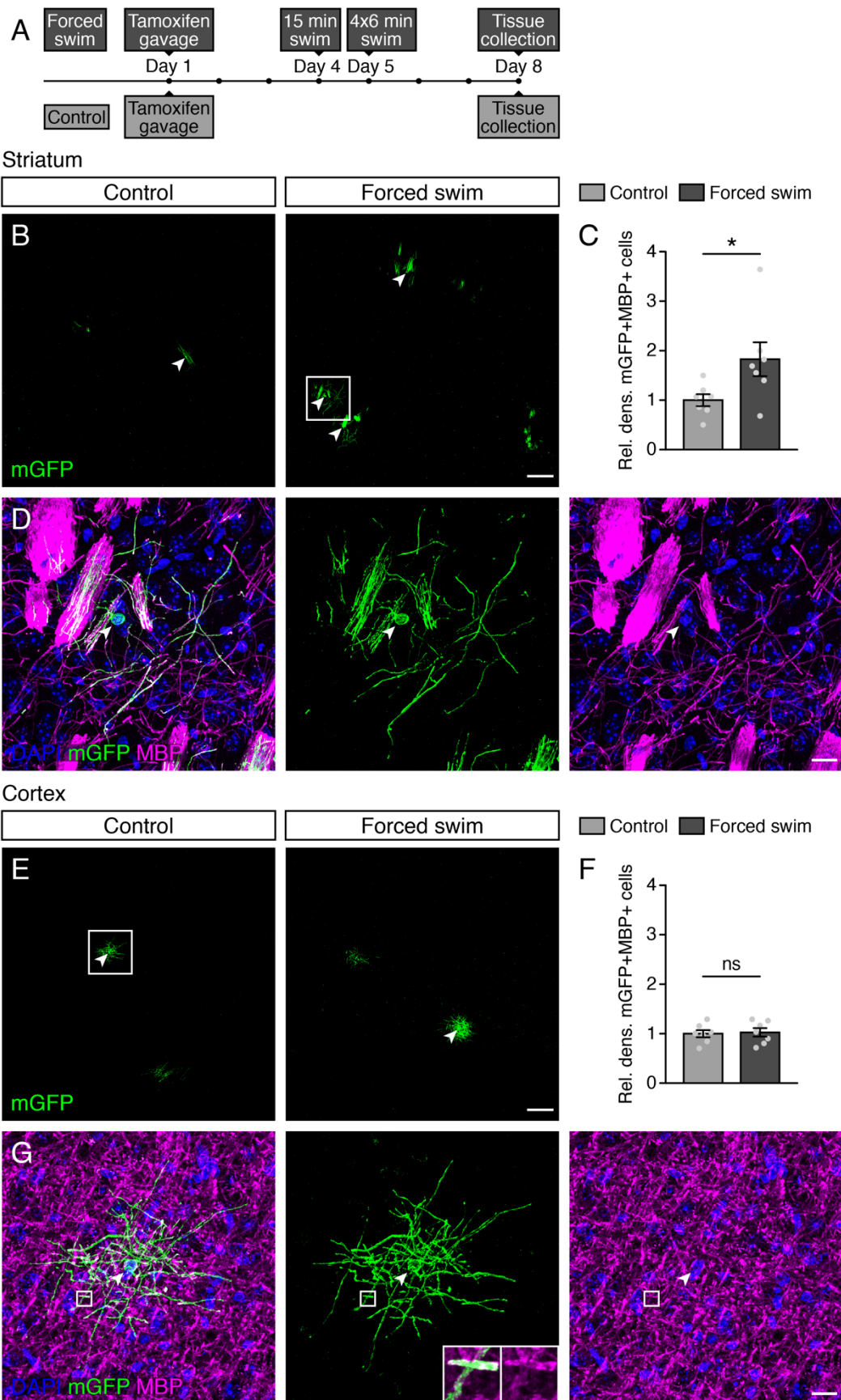
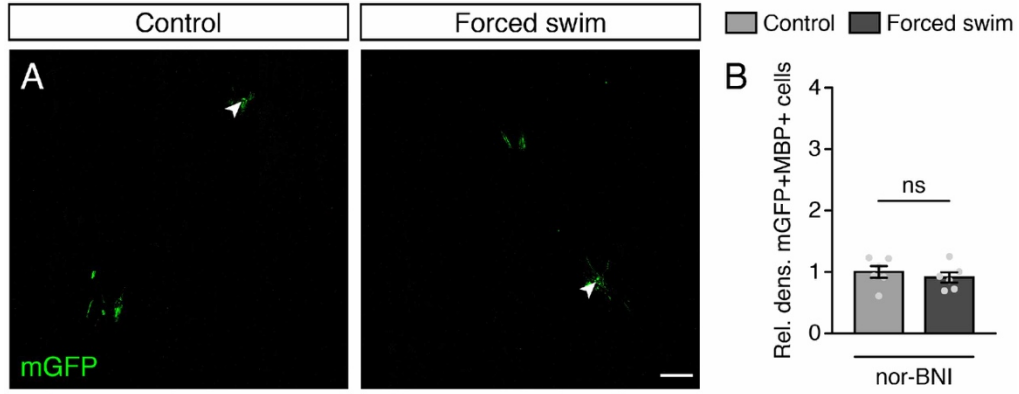


Figure 2.2: Forced swim stress promotes striatal OPC differentiation and myelination. (A) Experimental paradigm for tamoxifen administration, forced swim stress, and tissue collection performed in 12-16 week old *Cspg4-CreERTM*; *Mapt-mGFP* littermates. (B) Representative images of mGFP+ oligodendrocytes in control and forced swim stressed mice in striatum. Only mGFP+MBP+ cells with a cell soma visible in the section were quantified (arrowheads). Box is around cell enlarged in (D). (C) Quantification of relative density of mGFP+MBP+ cells in striatum in control versus forced swim stressed mice (both groups: n = 7; control: 1.000 ± 0.1202 , forced swim: 1.827 ± 0.3423 ; $P = 0.0418$, $t(12) = 2.379$). (D) Enlargement of a single mGFP+ oligodendrocyte from (B) colocalizing with DAPI and MBP. (E) Representative images in cortex. Box is around cell enlarged in (G). (F) Quantification in cortex (both groups: n = 7; control: 1.000 ± 0.07325 , forced swim: 1.026 ± 0.08559 ; $P = 0.8240$, $t(12) = 0.2274$). (G) Enlargement from (E). Box is around a mGFP+MBP+ myelin segment enlarged in 7.5 μm insets in the lower right corner of the center panel. Scale bars, (B) and (E), 100 μm ; (D) and (G), 15 μm . Data are presented as mean \pm s.e.m.; significance determined using two-tailed Student's t test; * $P < 0.05$; ns = not significant.

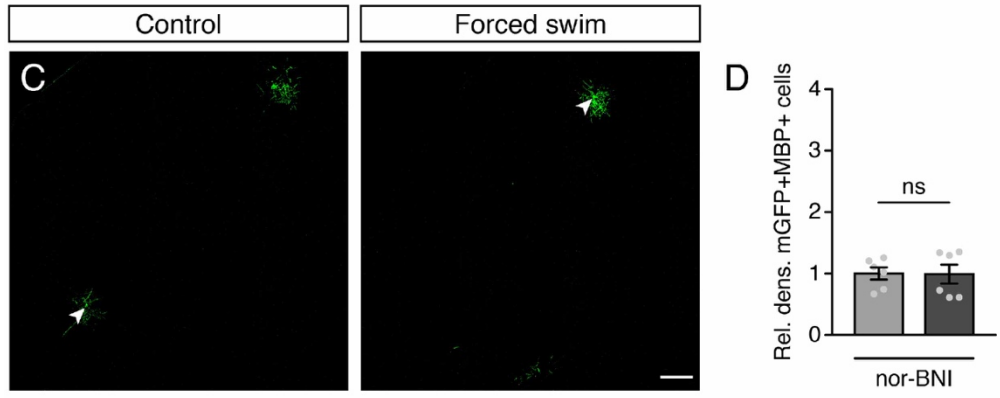
Stress-induced OPC differentiation is dynorphin-dependent

Since forced swim stress has been shown to cause striatal dynorphin release (Bruchas et al., 2008; Schindler et al., 2012) and activation of the endogenous dynorphin receptor, KOR, on OPCs promotes their differentiation (Du et al., 2016; Mei et al., 2016), we next investigated whether this experience-dependent myelination in response to acute stress was dependent on dynorphin signaling. To do this, we blocked dynorphin-KOR signaling by two methods. First, we used nor-Binaltorphimine dihydrochloride (nor-BNI), a highly selective, long-acting KOR antagonist that blocks dynorphin signaling (Horan et al., 1992; Portoghese et al., 1987). Nor-BNI blocks KOR agonists from promoting OPC differentiation (Mei et al., 2016) and prevents dynorphin-dependent behavioral outcomes of forced swim stress when administered 1 h prior to forced swim (McLaughlin et al., 2003). Using this same protocol, we injected *Cspg4-CreERTM*; *Mapt-mGFP* mice undergoing forced swim stress and their home cage littermate controls with nor-BNI 1 h

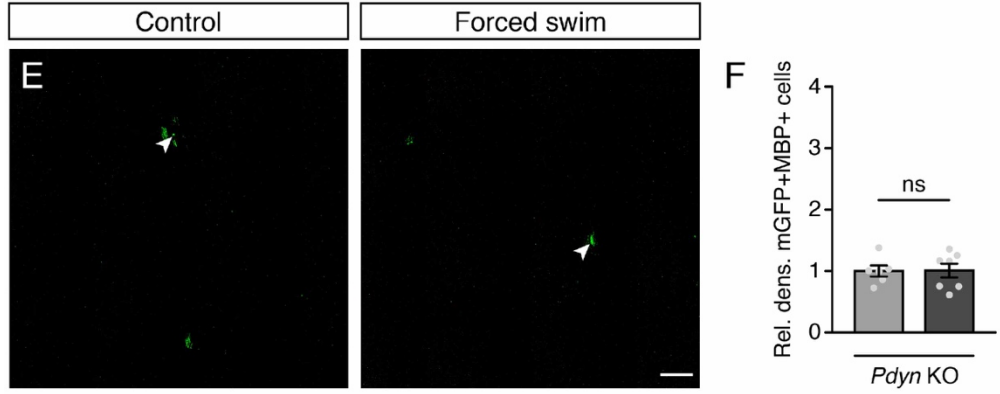
Striatum: nor-BNI



Cortex: nor-BNI



Striatum: *Pdyn* KO



Cortex: *Pdyn* KO

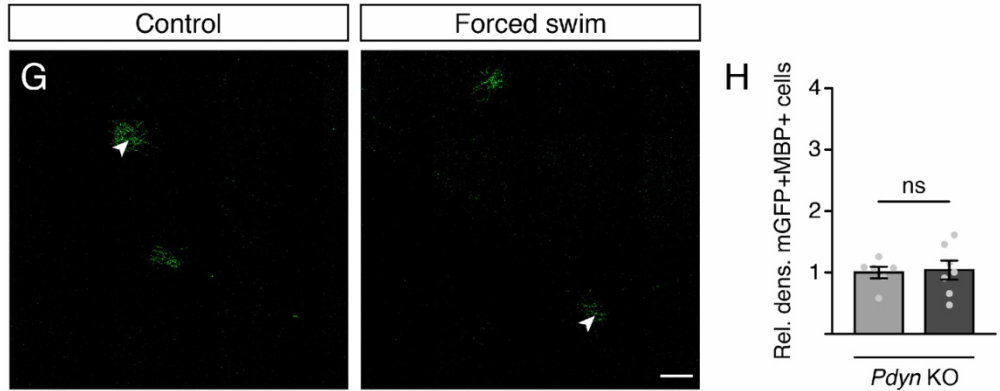


Figure 2.3: Blocking dynorphin-KOR signaling prevents stress-induced OPC differentiation and myelination. (A) Representative images of mGFP+ oligodendrocytes in striatum of control and forced swim stressed 12-16 week old *Cspg4-CreERTM*; *Mapt-mGFP* littermates given the KOR antagonist nor-BNI 1h prior to both sessions of forced swim stress. Only mGFP+MBP+ cells with a cell soma visible in the section were quantified (arrowheads). (B) Quantification of relative density of mGFP+MBP+ cells in striatum of mice described in (A) (both groups: n = 6; control: 1.000 ± 0.09525 , forced swim: 0.911 ± 0.08374 ; P = 0.4989, t(10) = 0.7016). (C) Representative images in cortex of mice described in (A). (D) Quantification in cortex of mice described in (A) (both groups: n = 6; control: 1.000 ± 0.09924 , forced swim: 0.9895 ± 0.1528 ; P = 0.9553, t(10) = 0.05751). (E) Representative images of mGFP+ oligodendrocytes in striatum of control and forced swim stressed 12-16 week old *Cspg4-CreERTM*; *Mapt-mGFP*; *Pdyn* KO littermates. (F) Quantification of relative density of mGFP+MBP+ cells in striatum of mice described in (E) (control: 1.000 ± 0.08924 , n = 6; forced swim: 1.008 ± 0.1113 , n = 7; P = 0.9579, t(11) = 0.05397). (G) Representative images in cortex of mice described in (E). (H) Quantification in cortex of mice described in (E) (control: 1.000 ± 0.0939 , n = 6; forced swim: 1.04 ± 0.1546 , n = 7; P = 0.8359, t(11) = 0.2121). Scale bars, 100 μ m. Data are presented as mean \pm s.e.m.; significance determined using two-tailed Student's t test; *P < 0.05; ns = not significant.

prior to the first forced swim trial on both days. We found that blocking dynorphin-KOR signaling prevented any stress-induced increase in mGFP+MBP+ myelinating oligodendrocytes in the striatum (**Figure 2.3 A, B**), whereas cortical OPC differentiation remained unaltered by forced swim stress (**Figure 2.3 C, D**).

Second, to eliminate dynorphin release, we crossed dynorphin (*Pdyn*) KO mice to *Cspg4-CreERTM*; *Mapt-mGFP* mice to generate *Cspg4-CreERTM*; *Mapt-mGFP*; *Pdyn* KO mice. *Cspg4-CreERTM*; *Mapt-mGFP*; *Pdyn* KO mice that underwent forced swim stress were compared to home cage littermate controls of the same genotype. Like with nor-BNI, we found that genetically eliminating dynorphin release prevented any stress-induced increase in striatal mGFP+MBP+ myelinating oligodendrocytes (**Figure 2.3 E, F**), whereas cortical OPC differentiation remained unaffected by forced swim stress (**Figure 2.3 G, H**). Together, these data demonstrate that forced swim stress-induced

striatal OPC differentiation and myelination requires dynorphin signaling, identifying dynorphin as a novel signal underlying experience-dependent myelination.

Dynorphin promotes developmental OPC differentiation and myelination

We next sought to determine whether dynorphin's role in myelination is limited to experience-dependent myelination following acute stress or whether it affects myelination more broadly. We previously observed a deficit in developmental OPC differentiation and myelination in mice lacking KOR on OPCs (*Olig2-Cre/+; Oprk1 flox/flox*, henceforth KOR cKO mice) (Mei et al., 2016), suggesting that dynorphin, the endogenous KOR agonist, may promote developmental OPC differentiation and myelination. To test this, we assessed *Pdyn* knock-out (KO) mice at the earliest stage of developmental myelination in the brain at postnatal day 8. By immunostaining, we observed a 23% decrease in the area occupied by the myelin protein MBP globally across cortex, corpus callosum, and striatum in *Pdyn* KO mice as compared to wild-type littermate controls (**Figure 2.4 A, B**). Since we previously showed that activating KOR on OPCs promotes their differentiation (Mei et al., 2016) and we found that dynorphin promotes OPC differentiation following stress (**Figure 2.2** and **Figure 2.3**), we hypothesized that the deficit in developmental myelination in *Pdyn* KO mice was due to a decrease in OPC differentiation. Consistent with our hypothesis, we observed a corresponding decrease in the density of oligodendrocytes (CC1+MBP+Olig2+ cells) in *Pdyn* KO mice (**Figure 2.4 C, D**) but no change in the density of total oligodendrocyte lineage cells (Olig2+ cells) (**Figure 2.4 C, E**), indicating a specific deficit in OPC differentiation. Together, these results indicate that dynorphin promotes OPC differentiation and myelination in development.

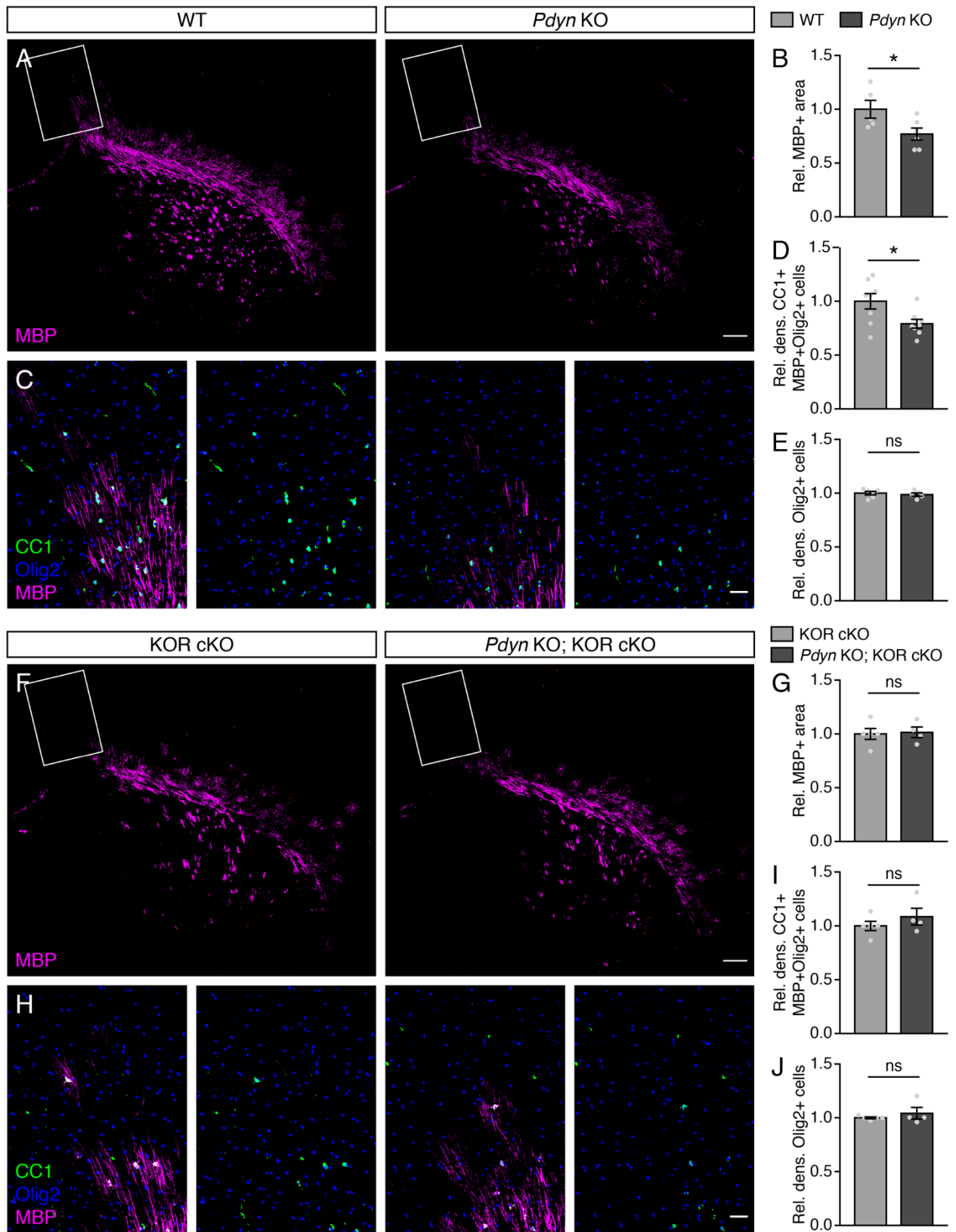


Figure 2.4: Dynorphin knock-out mice have deficits in developmental OPC differentiation and myelination redundant with the loss of OPC KORs. (A) Representative images of MBP immunostaining in the quantification region for MBP area encompassing cortex, corpus callosum, and striatum in postnatal day (P) 8 wild-type (WT) and *Pdyn* KO littermates. The box in cortex corresponds to the quantification region for CC1+MBP+ Olig2+ and Olig2+ cells in (C). **(B)** Quantification of relative MBP area in P8 WT and *Pdyn* KO littermates (WT: 1.000 ± 0.08261 , $n = 5$; *Pdyn* KO: 0.7693 ± 0.05614 , $n = 6$; $P = 0.0414$, $t(9) = 2.478$). **(C)** Representative images of MBP, CC1, and Olig2 immunostaining in the quantification region for CC1+MBP+Olig2+ and Olig2+ cells in P8 WT and *Pdyn* KO littermates. **(D, E)** Quantification of relative density of CC1+MBP+ Olig2+ cells (both groups: $n = 8$; WT: 1.0000 ± 0.07106 , *Pdyn* KO: 0.7914 ± 0.04061 ; $P = 0.0232$, $t(14) = 2.548$) (D) and relative density of Olig2+ cells (WT: 1.0000 ± 0.01643 , $n = 6$; *Pdyn* KO: 0.9866 ± 0.01563 , $n = 5$; $P = 0.5754$, $t(9) = 0.5812$) (E) in P8 WT and *Pdyn* KO littermates. **(F)** Representative images of MBP immunostaining in P8 KOR cKO and *Pdyn* KO; KOR cKO littermates. **(G)** Quantification of relative MBP area in P8 KOR cKO and *Pdyn* KO; KOR cKO littermates (KOR cKO: 1.000 ± 0.05024 , $n = 5$; *Pdyn* KO; KOR cKO: 1.015 ± 0.0493 , $n = 4$; $P = 0.8445$, $t(7) = t = 0.2036$). **(H)** Representative images of MBP, CC1, and Olig2 immunostaining in the quantification region for CC1+MBP+Olig2+ and Olig2+ cells in P8 KOR cKO and *Pdyn* KO; KOR cKO littermates. **(I, J)** Quantification of relative density of CC1+MBP+Olig2+ cells (KOR cKO: 1.000 ± 0.04294 , $n = 5$; *Pdyn* KO; KOR cKO: 1.086 ± 0.07834 , $n = 4$; $P = 0.3406$, $t(7) = 1.022$) (D) and relative density of Olig2+ cells (KOR cKO: 1.000 ± 0.007635 , $n = 5$; *Pdyn* KO; KOR cKO: 1.042 ± 0.05419 , $n = 4$; $P = 0.4119$, $t(7) = 0.8724$) (E) in P8 KOR cKO and *Pdyn* KO; KOR cKO littermates. Scale bars, (A) and (F), 200 μm ; (C) and (H) 50 μm . Data are presented as mean \pm s.e.m.; significance determined using two-tailed Student's t test; * $P < 0.05$; ns = not significant.

Dynorphin acts through OPC KORs to promote OPC differentiation and myelination

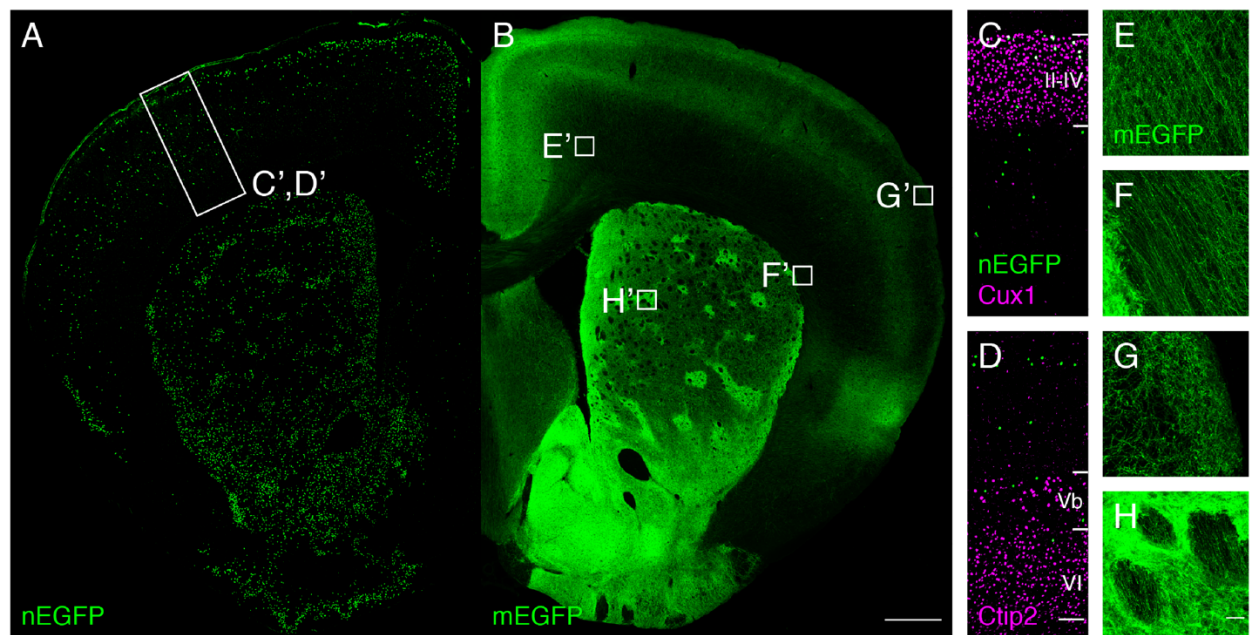
Our finding that *Pdyn* KO mice phenocopy the developmental deficits in OPC differentiation and myelination observed in KOR cKO mice suggests that dynorphin acts through KORs on OPCs to promote OPC differentiation and myelination. To directly test this hypothesis, we examined whether the deficits in developmental OPC differentiation and myelination induced by *Pdyn* KO mice and KOR cKO mice were additive or redundant. We crossed *Pdyn* KO mice into KOR cKO mice to generate *Pdyn* KO; KOR cKO (*Pdyn* KO; *Olig2-Cre/+*; *Oprk1* flox/flox) and KOR cKO (*Olig2-Cre/+*; *Oprk1* flox/flox) littermates and compared them at postnatal day 8. If dynorphin acts independent of OPC

KORs to promote developmental OPC differentiation and myelination, we would expect mice lacking both dynorphin and OPC KORs to display a further deficit in developmental OPC differentiation and myelination than do mice lacking OPC KORs alone. Conversely, if dynorphin acts through OPC KORs to promote developmental OPC differentiation and myelination, the deletion of dynorphin would be redundant with the deletion of OPC KORs and we should observe no difference between these groups. Consistent with the latter hypothesis, we observed no difference in MBP area between *Pdyn* KO; KOR cKO mice and KOR cKO littermates (**Figure 2.4 F, G**). Furthermore, we observed no difference in the density of oligodendrocytes (CC1+MBP+Olig2+ cells) (**Figure 2.4 H, I**) or total oligodendrocyte lineage cells (Olig2+) (**Figure 2.4 H, J**) between *Pdyn* KO; KOR cKO mice and KOR cKO littermates. Together, these data indicate that dynorphin acts through OPC KORs to induce OPC differentiation and myelination.

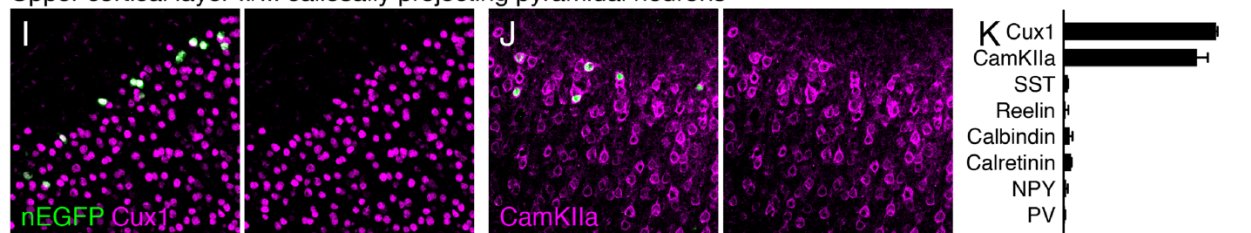
Dynorphin is expressed in a subset of neurons

As the activity of multiple different neuronal subtypes has been implicated in regulating OPC differentiation and myelination (Gibson et al., 2014; Mitew et al., 2018), we sought to identify the neuronal subtypes expressing dynorphin. To visualize dynorphin-expressing cells, we crossed *Pdyn-Cre* mice with nTnG mice or mTmG mice, generating *Pdyn-Cre*; nTnG and *Pdyn-Cre*; mTmG mice, where Cre-dependent recombination in dynorphin-expressing cells replaces tdTomato fluorescence with nuclear EGFP or membrane EGFP expression, respectively. In *Pdyn-Cre*; nTnG mice, we observed widespread EGFP+ nuclei in the striatum and cortex (**Figure 2.5 A**). The cortical EGFP+ nuclei were distributed in two populations whose positions could be localized using the

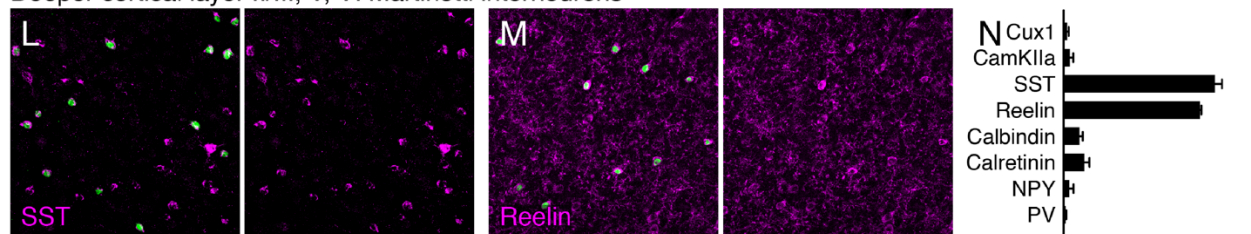
cortical layer markers Cux1 for layer II-IV (**Figure 2.5 C**) and Ctip2 for layers Vb/VI (**Figure 2.5 D**). One population was tightly clustered in upper layer II/III (Figures 2.5 A, C). The other population was more broadly distributed in the deeper cortical layers, with



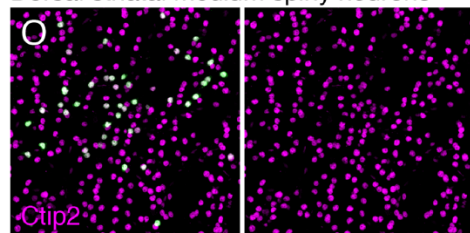
Upper cortical layer II/III callosally projecting pyramidal neurons



Deeper cortical layer II/III, V, VI Martinotti interneurons



Dorsal striatal medium spiny neurons



Ventral striatal medium spiny neurons

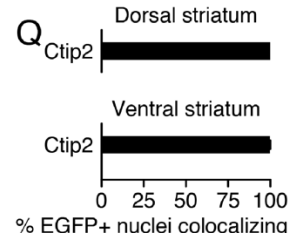
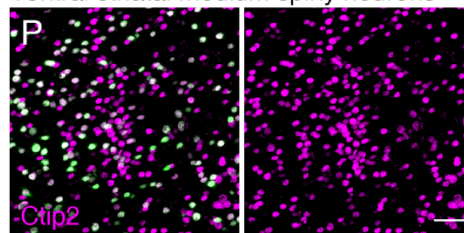


Figure 2.5: Identification of several neuronal subtypes expressing dynorphin. (A, B) Representative images of nEGFP (A) and mEGFP (B) immunostaining in half coronal sections of 12-16 week old *Pdyn-Cre*; nTnG (A) or *Pdyn-Cre*; mTmG (B) mice. Boxes refer to the regions enlarged in (C-H). **(C, D)** Representative images showing localization of one population of nEGFP+ cells in upper cortical layer II/III and another spread throughout deeper cortical layers, localized by the layer II-IV marker *Cux1* (C) and the layer Vb-VI marker *Ctip2* (D). **(E-H)** Representative images of mEGFP+ axon tracts in cortical layer VI (E), corpus callosum (F), cortical layer I (G), and striatum (H). **(I, J)** Representative images showing colocalization of upper layer II/III nEGFP+ cells with pyramidal neuron markers *Cux1* (I) and *CamKIIa* (J). **(K)** Quantification of the percentage of upper cortical layer II/III nEGFP+ cells colocalizing with neuronal markers in $n = 2$ mice. **(L, M)** Representative images showing colocalization of deeper cortical layer nEGFP+ cells with markers for Martinotti cells, somatostatin (SST) (L) and reelin (M). **(N)** Quantification the percentage of deeper cortical layer nEGFP+ cells colocalizing with neuronal markers in $n = 2$ mice. **(O, P)** Representative images showing colocalization of dorsal (O) and ventral (P) striatal nEGFP+ cells with medium spiny neuron marker *Ctip2*. **(Q)** Quantification of percentage of striatal nEGFP+ cells colocalizing with *Ctip2* in $n = 2$ mice. Abbreviations: NPY = neuropeptide Y; PV = parvalbumin. Scale bars, (A) and (B), 500 μm ; (C) and (D), 100 μm ; (E-H), 20 μm ; (I), (J), (L), (M), (O), and (P), 50 μm . Data are presented as mean \pm s.d.

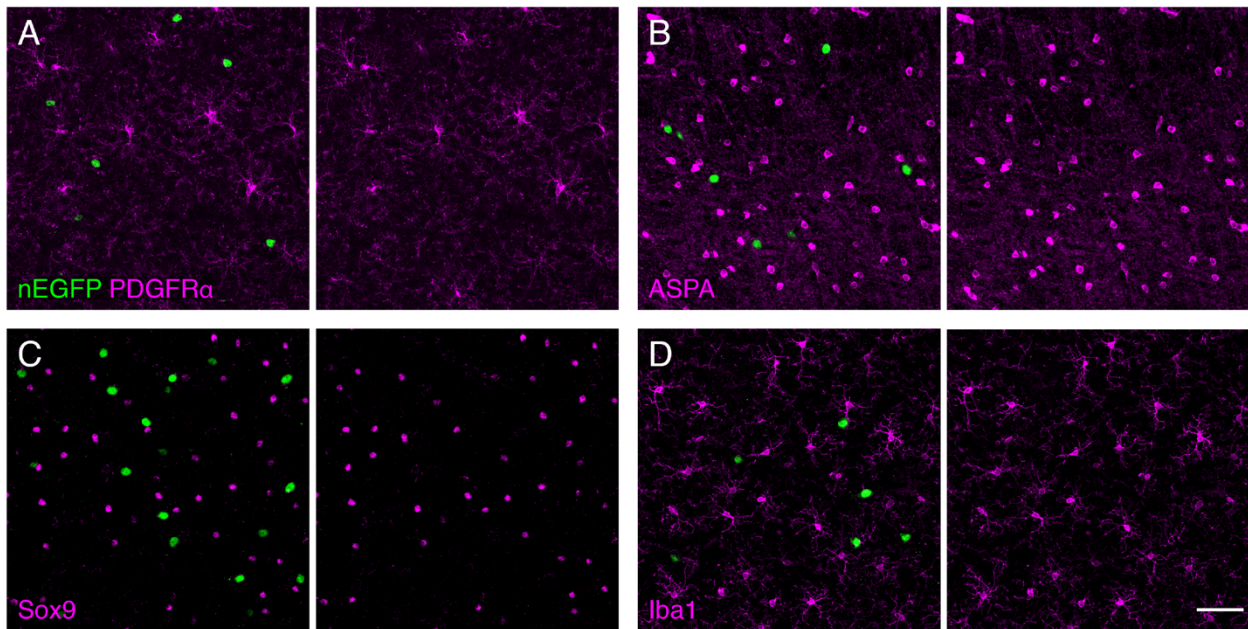


Figure 2.6: Dynorphin is not expressed in glia. (A-D) Representative images of immunostaining in 12-16 week old *Pdyn-Cre*; nTnG mice showing no colocalization between nEGFP+ cells and markers for OPCs (A), oligodendrocytes (B), astrocytes (C), or microglia (D) in deeper cortical layers. Scale bars, 50 μm .

the majority in layer V and some in the deeper part of layers II-IV or in layer VI (**Figure 2.5 A, C, D**). In *Pdyn-Cre*; mTnG mice, the distribution of dynorphin-expressing cells observed in *Pdyn-Cre*; nTnG mice was replicated and furthermore, the processes of dynorphin-expressing cells could be visualized (**Figure 2.5 B**). Tracts of mEGFP+ axons projecting towards or away from (**Figure 2.5 E**) and within (**Figure 2.5 F**) the corpus callosum could be observed, as well as mEGFP+ axons elaborating in layer I (**Figure 2.5**

Upper cortical layer II/III

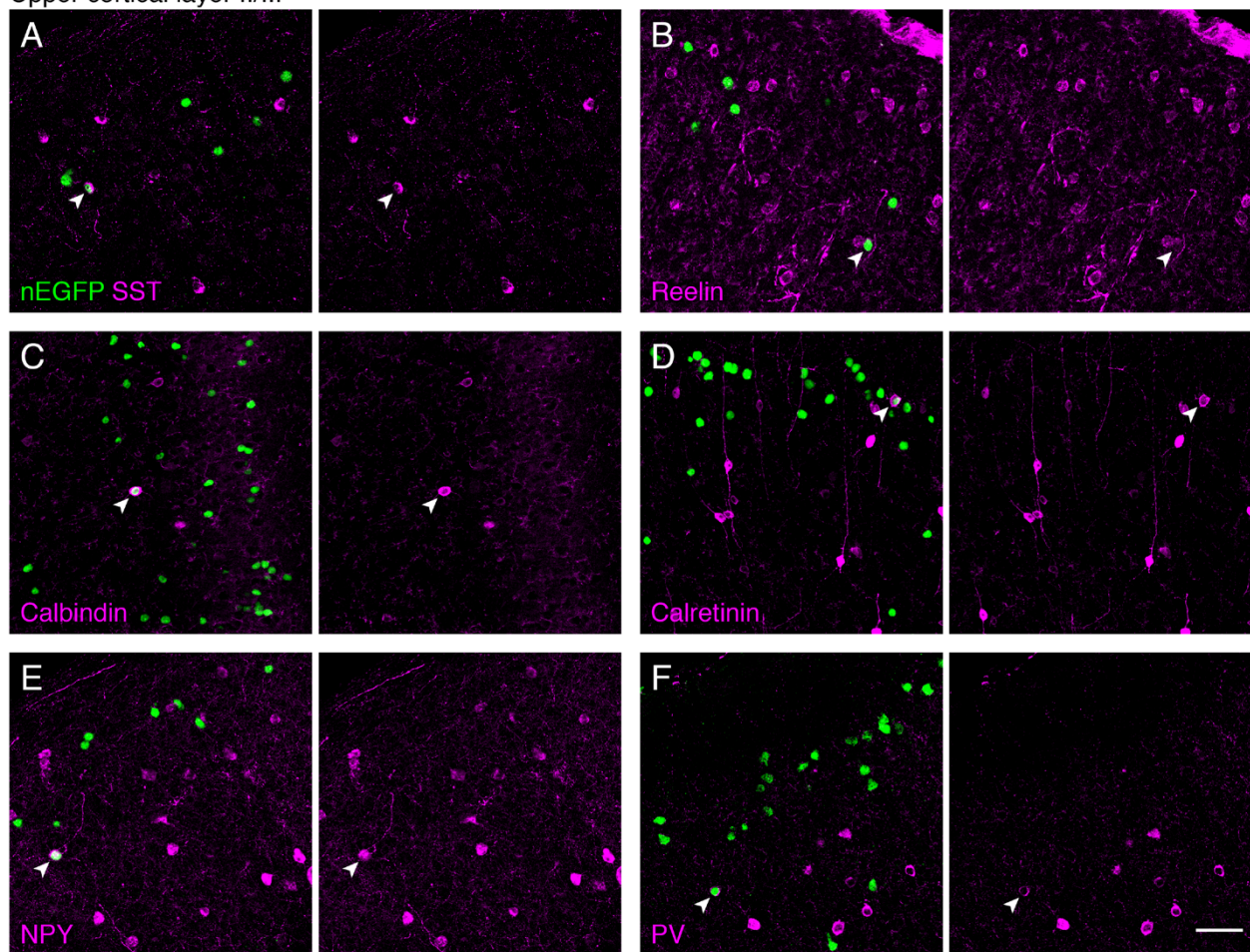


Figure 2.7: Upper cortical layer II/III dynorphin-expressing cells rarely colocalize with interneuron markers. (A-F) Representative images of immunostaining in 12-16 week old *Pdyn-Cre*; nTnG mice in upper cortical layer II/III showing rare examples of colocalization between nEGFP+ cells and interneuron markers somatostatin (SST) (A), reelin (B), calbindin (C), calretinin (D), neuropeptide Y (NPY) (E), and parvalbumin (PV) (F). Examples of colocalization are indicated with an arrowhead. Scale bars, 50 μ m.

G) and projecting in striatal axon bundles (**Figure 2.5 H**).

To identify the cell types expressing dynorphin, we examined colocalization of EGFP+ nuclei in *Pdyn-Cre*; nTnG mice with various markers. We did not observe any colocalization with glial markers for OPCs, oligodendrocytes, astrocytes, or microglia

Deeper cortical layers II/III, V, VI

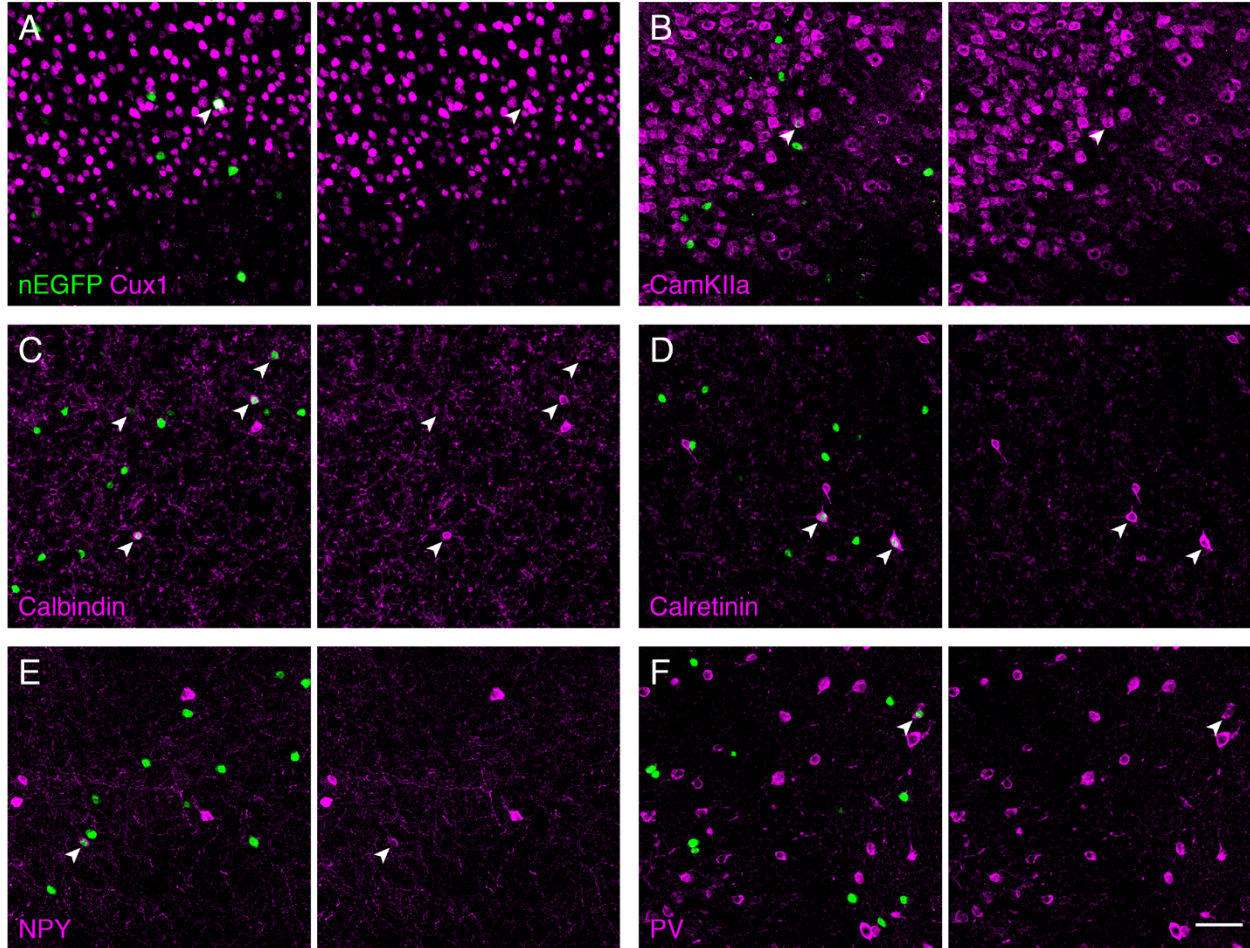


Figure 2.8: Deeper cortical layer dynorphin-expressing cells rarely colocalize with non-Martinotti cell markers. (A-F) Representative images of immunostaining in 12-16 week old *Pdyn-Cre*; nTnG mice in deeper cortical layers showing rare examples of colocalization between nEGFP+ cells and pyramidal neuron markers Cux1 (A) and CamKIIa (B), occasional colocalization with markers sometimes expressed in Martinotti cells calbindin (C) and calretinin (D), but rare colocalization with another marker sometimes expressed in Martinotti cells neuropeptide Y (NPY) (E), or a non-Martinotti interneuron marker parvalbumin (PV) (F). Examples of colocalization are indicated with arrowheads. Scale bars, 50 μ m.

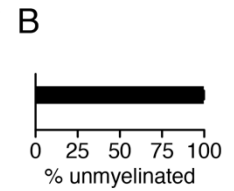
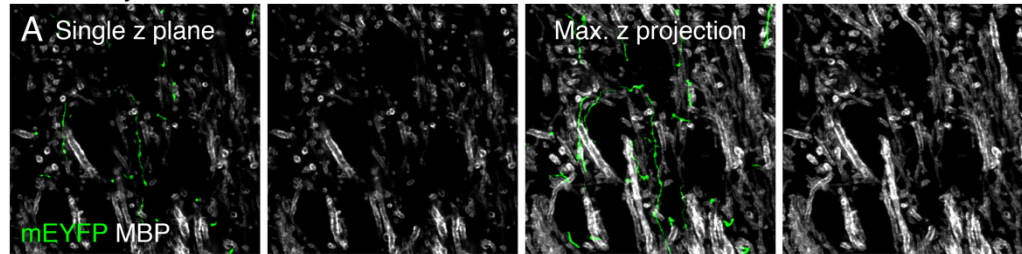
(**Figure 2.6 A-D**). The upper layer II/III EGFP+ nuclei colocalized with pyramidal neuron markers Cux1 and CamKIIa (**Figure 2.5 I-K**) and rarely colocalized with interneuron markers (**Figures 2.5 K** and **Figure 2.7 A-F**), indicating that this dynorphin-expressing neuronal population is made up of layer II/III pyramidal neurons, which project through the corpus callosum (**Figure 2.5 E, F**) to innervate the contralateral cortex. The EGFP+ nuclei in the deeper cortical layers primarily colocalized with somatostatin (SST) and reelin, and to a much lesser extent calbindin and calretinin (**Figure 2.5 L-N** and **Figure 2.8 A-F**), in agreement with a previous report (Sohn et al., 2014). This molecular profile is suggestive of Martinotti cells, interneurons predominantly localized to layer V but also found in layers II/III and VI, which project their axons into layer I (Tremblay et al., 2016). These deeper cortical layer dynorphin-expressing neurons matched this cortical distribution (**Figure 2.5 A, C, D**) and their mEGFP+ axonal ramifications were observable throughout layer I (**Figure 2.5 G**), indicating these cells are indeed Martinotti cells. Finally, as expected, all EGFP+ nuclei in the striatum colocalized with Ctip2 (**Figure 2.5 O-Q**), a marker for medium spiny neurons, as striatal dynorphin-expressing neurons are known to be direct-pathway medium spiny neurons (Gerfen et al., 1990). Collectively, these results identify three populations of dynorphin-expressing neurons throughout the cortex and striatum.

Axons of dynorphin-expressing neurons are unmyelinated

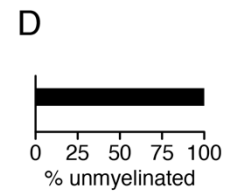
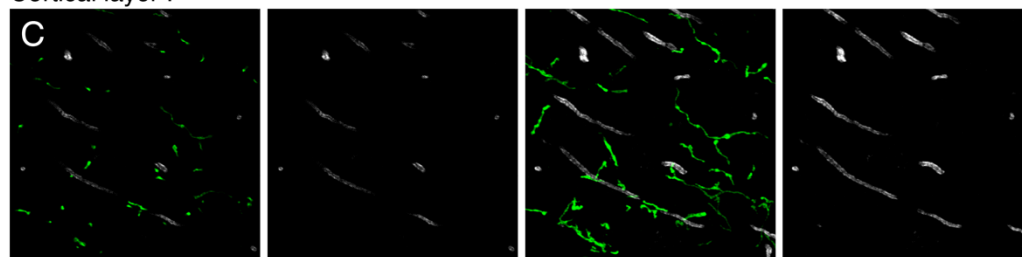
Not all axons in the brain are myelinated and many axons are only partially myelinated (Micheva et al., 2016; Sturrock, 1980; Tomassy et al., 2014), but how axons are selected for myelination remains an outstanding question. A recent study showed that increased

activity of layer II/III pyramidal neurons promotes OPC differentiation and myelination as well as the targeting of this new myelin to those activated pyramidal axons (Mitew et al.,

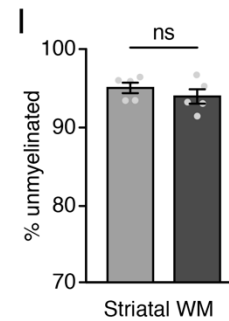
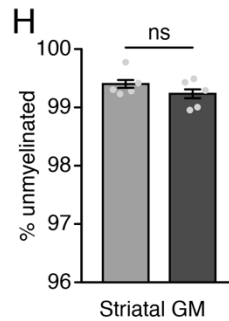
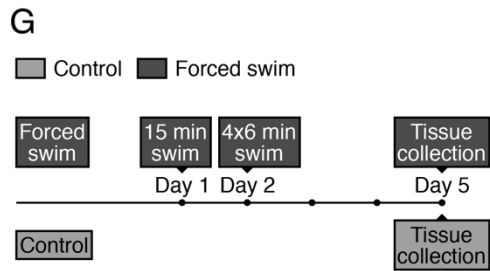
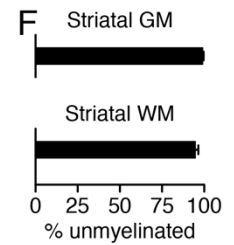
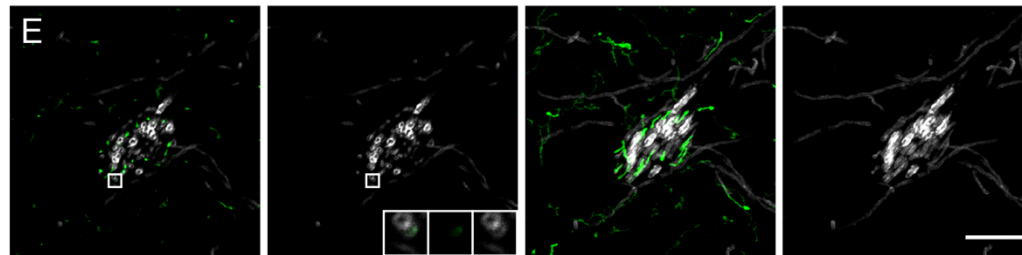
Cortical layer VI



Cortical layer I



Striatum: Control



Striatum: Forced swim

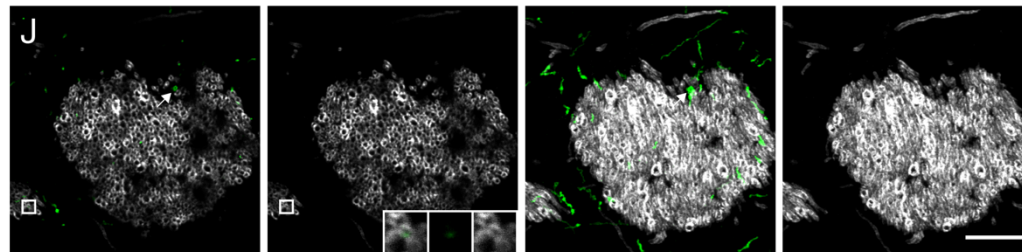


Figure 2.9: Axons of dynorphin-expressing neurons are unmyelinated normally and following forced swim stress. (A) Representative images of immunostaining for mEYFP and MBP in cortical layer VI in 12-16 weeks old *Pdyn-Cre*; STARS mice. Left: at the resolution of a single z plane, the colocalization of mEYFP and MBP can readily be assessed; right: 6 μm depth maximum intensity z projections of the same images. (B) Quantification of percentage of unmyelinated mEYFP+ axons in cortical layer VI (3950/3960 axons, n = 3 mice) of mice described in (A). (C) Representative images of cortical layer I as described in (A). (D) Quantification in cortical layer I (5549/5549 axons, n = 3 mice) as described in (B). (E) Representative images of striatum as described in (A). Box is around a myelinated mEYFP+ axon enlarged in 4 μm insets in the lower right corner of the center-left panel. (F) Quantification in striatal gray matter (8902/8967 axons, n = 5 mice) and white matter (1457/1543 axons, n = 5 mice) as described in (B). (G) Experimental paradigm for forced swim stress and tissue collection performed in 12-16 week old *Pdyn-Cre*; STARS littermates. (H, I) Quantification of percentage of unmyelinated mEYFP+ axons in control and forced swim stressed littermates in striatal gray matter (both groups: n = 5, control: 99.4 ± 0.09768 , forced swim: 99.24 ± 0.1094 ; P = 0.2863, t(8) = 1.143) (H) and white matter (both groups: n = 5, control: 95.01 ± 0.6661 , forced swim: 93.91 ± 0.9236 ; P = 0.3601, t(8) = 0.9707) (I). (J) Representative images of immunostaining for mEYFP and MBP in striatum of 12-16 weeks old forced swim stressed *Pdyn-Cre*; STARS mice. Box is around a myelinated mEYFP+ axon enlarged in 4 μm insets in the lower right corner of the center-left panel. mEYFP+ dendrites (arrow) were readily identifiable in all regions by their larger diameter and the presence of spines. Dendrites were excluded from quantification. Scale bars, 20 μm . Data in (B), (D), and (F) are presented as mean \pm s.d.; data in (H, I) presented as mean \pm s.e.m.; significance determined using two-tailed Student's t test; *P < 0.05; ns = not significant.

2018). However, it is unknown which signaling mechanisms regulate this process, and whether the same axonal signal could both promote OPC differentiation and targeting of the resulting myelin to the source axon. Other studies have shown that the selection of axons for myelination is promoted by neuronal vesicular release (Hines et al., 2015; Koudelka et al., 2016). These findings led us to ask whether dynorphin, in addition to its role in promoting OPC differentiation, could also promote the selection of dynorphin-expressing neurons for myelination. To test this possibility, we examined whether the axons of dynorphin-expressing neurons were myelinated. The high density of mEGFP+ axons throughout the brain (Figure 2.5 B, E-H) prevented us from being able to readily distinguish individual axons in *Pdyn-Cre*; mTmG mice by immunofluorescence.

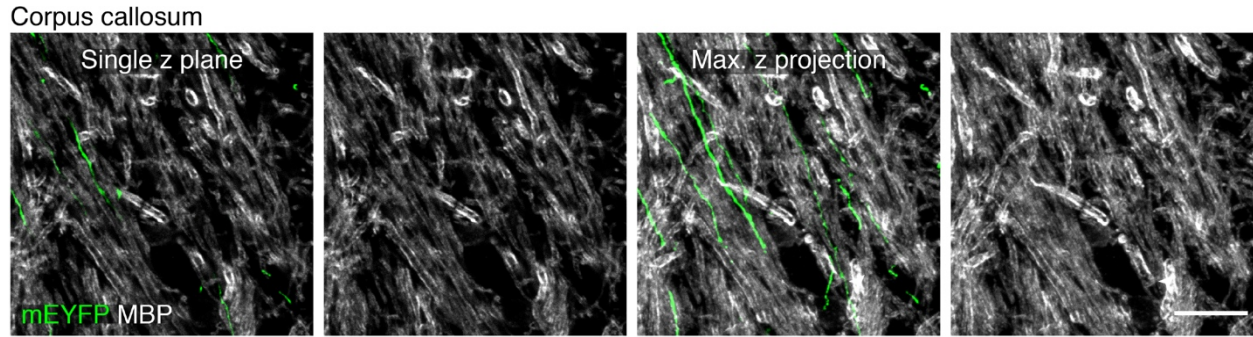


Figure 2.10: Axons of dynorphin-expressing neurons in the corpus callosum are unmyelinated. Representative images of immunostaining for mEYFP and MBP in corpus callosum in 12-16 weeks old *Pdyn-Cre*; STARS mice. Left: single z plane; right: 6 μm depth maximum intensity z projection. Scale bar, 20 μm .

Therefore, we turned to a novel method for sparsely labeling cells: the STARS (stochastic gene activation with regulated sparseness) reporter mouse. A single copy of the STARS transgene allows for membrane EYFP (mEYFP) expression in only 10% of Cre-expressing cells (Ibrahim et al., 2018). We crossed *Pdyn-Cre* mice with STARS mice to generate *Pdyn-Cre*; STARS mice, which allowed us to assess the myelination status of individual dynorphin-expressing axons in several regions using confocal microscopy (**Figure 2.9 A, C, E** and **Figure 2.10**). Looking for colocalization of mEYFP+ axons and MBP+ myelin, we found that the axons of dynorphin-expressing neurons were overwhelmingly unmyelinated in all regions observed (**Figure 2.9 A-F** and **Figure 2.10**). The axons of dynorphin-expressing layer II/III pyramidal neurons were unmyelinated in cortical layer VI (99.76%; **Figure 2.9 A, B**) and in the corpus callosum (**Figure 2.10**). The axons of dynorphin-expressing Martinotti cells were unmyelinated in cortical layer I (100%; **Figure 2.9 C, D**). Finally, in the striatum, axons of dynorphin-expressing neurons were unmyelinated in the neuropil (gray matter: 99.40%) and axon tracts (white matter:

95.01%; **Figure 2.9 E, F**). Together, these data indicate that dynorphin does not promote the myelination of dynorphin-expressing axons over the course of normal development.

Dynorphin-expressing neurons remain unmyelinated following forced swim stress

Although the axons of dynorphin-expressing neurons were unmyelinated under baseline conditions, we hypothesized that an experience like forced swim stress, which induces dynorphin release (Bruchas et al., 2008; Schindler et al., 2012) and increases OPC differentiation (**Figure 2.2** and **Figure 2.3**), could promote their myelination. Using the same paradigm of forced swim stress that promoted striatal OPC differentiation and myelination (**Figure 2.2 A** and **Figure 2.9 G**), we tested whether forced swim stress would promote the myelination of dynorphin expressing neurons in the striatum. We found that forced swim stress did not alter the percentage of unmyelinated mEYFP+ axons in the gray matter (**Figure 2.9 H, J**) or white matter of the striatum (**Figure 2.9 I, J**). These results indicate that following forced swim stress – like at baseline – dynorphin does not promote the myelination of dynorphin-expressing axons.

Small axonal diameter contributes to low myelination rates of dynorphin-expressing neurons

In quantifying the percentage of myelinated mEYFP+ axons, we observed that they appeared to be of noticeably smaller diameter than the MBP+ myelin segments in the same regions (**Figure 2.9 A, C, E** and **Figure 2.10**). It is well-accepted that axons with a diameter smaller than roughly 0.3 μm are unable to be myelinated by oligodendrocytes (Lee et al., 2012) and previous work has shown that cortical SST+ Martinotti cells – a

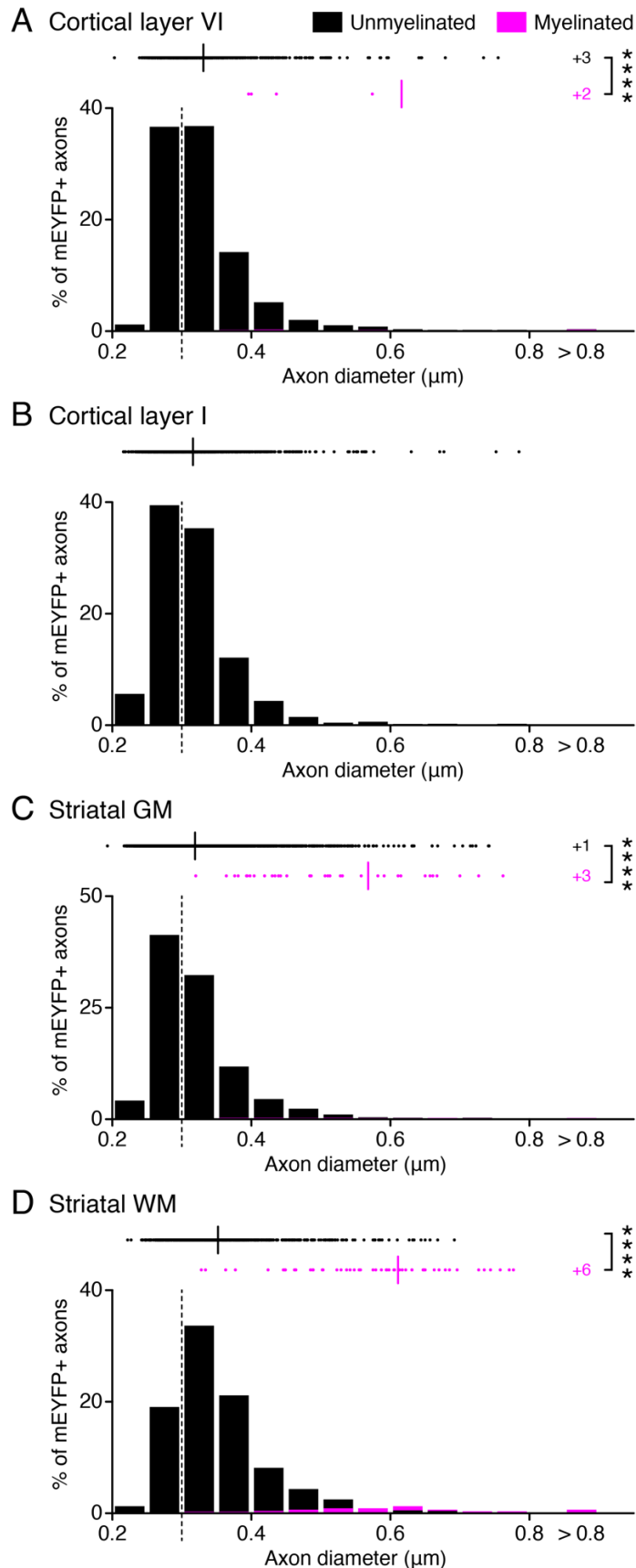


Figure 2.11: Dynorphin-expressing neurons have small diameter axons. (A) Top: Aligned dot plot with mean of axon diameters of unmyelinated (black) and myelinated (magenta) mEYFP+ axons in cortical layer VI (unmyelinated: median = 0.3128, n = 817 axons; myelinated: median = 0.5056, n = 6 axons; U = 240, P < 0.0001). Bottom: Histogram of the same data binned into 0.05 μm bins. The myelination threshold for oligodendrocytes at 0.3 μm is indicated by a dotted line. (B) Top: Aligned dot plot with mean of axon diameters of unmyelinated mEYFP+ axons in cortical layer I (n = 1259 axons). Bottom: Histogram as described in (A) of cortical layer I. (C) Top: Aligned dot plot as described in (A) of striatal GM (unmyelinated: median = 0.3051, n = 3259 axons; myelinated: median = 0.5123, n = 36 axons; U = 5466, P < 0.0001). Bottom: Histogram as described in (A) of striatal GM. (D) Top: Aligned dot plot as described in (A) of striatal WM (unmyelinated: median = 0.3402, n = 756 axons; myelinated: median = 0.5987, n = 59 axons; U = 2342, P < 0.0001). Bottom: Histogram as described in (A) of striatal WM. Data points > 0.8 μm are summed at the right-most side of the graphs. Significance determined using two-tailed Mann-Whitney test; **** P < 0.0001.

subset of which express dynorphin (**Figure 2.5 L-N**) – are unmyelinated due to their small axonal diameters (Stedehouder et al., 2019). This led us to interrogate whether the axons of dynorphin-expressing neurons may remain unmyelinated due to size. We estimated axon diameters by measuring the full-width at half maximum (FWHM) of mEYFP fluorescence intensity across axons, as previously described (Call and Bergles, 2021; Stedehouder et al., 2019), in cortex and striatum. Across the regions, a substantial percentage of unmyelinated mEYFP+ axons were below 0.3 μm in diameter and thus were unable to be myelinated (cortical layer VI: 38.19%; cortical layer I: 45.12%; striatal GM: 46.15%; striatal WM: 22.09%), and the vast majority were below 0.4 μm in diameter (cortical layer VI: 89.60%; cortical layer I: 92.61%; striatal GM: 90.83%; striatal WM: 81.35%) (**Figure 2.11 A-D**).

We also measured the diameters of the few mEYFP+ axons that were myelinated. On average, we found that myelinated mEYFP+ axons were larger than unmyelinated mEYFP+ axons in all regions where we observed mEYFP+ axon myelination (**Figure 2.11 A, C, D**). When considering only suprathreshold axons, diameter still influenced myelination status. mEYFP+ axons larger than 0.5 μm had substantially higher rates of myelination (cortical layer VI: 10.71%; striatal GM: 22.47%; striatal WM: 54.22%) than those between 0.3 μm and 0.5 μm (cortical layer VI: 0.62%; striatal GM: 0.94%; striatal WM: 2.48%) in all regions where we observed mEYFP+ axon myelination. Together, these data indicate that small axon size indeed contributes to the extremely low myelination rate of dynorphin-expressing neurons.

However, small axonal diameter does not entirely account for the low myelination rate of dynorphin-expressing neurons. Even when compared across the same axon size,

the myelination rate of dynorphin-expressing neurons is substantially lower than that of other CNS neuronal subtypes. Below 0.5 μm , the axons of dynorphin-expressing neurons are almost entirely unmyelinated (cortical layer VI: 0.38%; cortical layer I: 0%; striatal GM: 0.50%; striatal WM: 1.91%), while cortical parvalbumin neurons and thalamocortically projecting ventral medial nucleus neurons are myelinated at rates of 30% and 21%, respectively (Call and Bergles, 2021). Clearly – in addition to small axonal diameter – there are other, yet defined factors that also contribute to preventing the myelination of dynorphin-expressing neurons.

2.4 Discussion

Overall, we identify the neuropeptide dynorphin as a neuronal signal promoting experience-dependent OPC differentiation and myelination following acute stress (**Figure 2.2** and **Figure 2.3**). Dynorphin also promotes developmental OPC differentiation and myelination (**Figure 2.4** A-E) and exerts its pro-differentiation effects by acting on OPC KORs (**Figure 2.4** F-J). Intriguingly, we found that the axons of dynorphin-expressing neurons are unmyelinated both under normal conditions (**Figure 2.9** A-F and **Figure 2.10**) and following acute stress (**Figure 2.9** H-J), which can be partially attributed to their small size (**Figure 2.11**). Based on our findings, we propose the following model wherein unmyelinated, dynorphin-expressing neurons influence the myelination of neighboring axons during development and following acutely stressful experiences by releasing dynorphin to induce OPC differentiation (**Figure 2.12**).

Over the last decade, it is has become increasingly clear that CNS myelination is sensitive to extrinsic cues. Several recent studies have shown that experience can

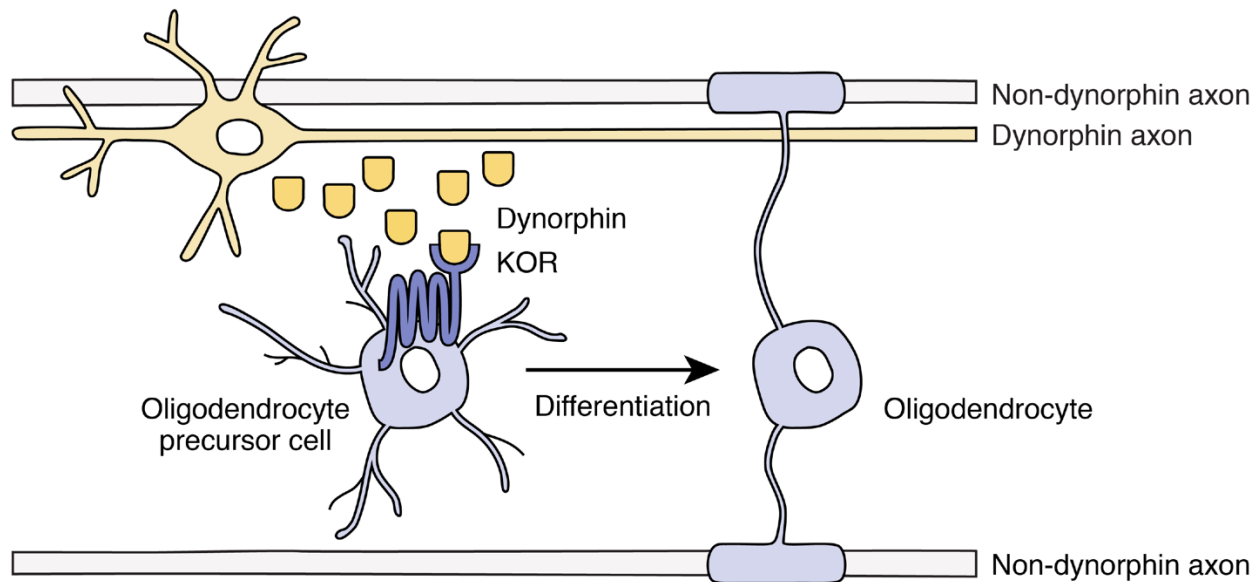


Figure 2.12: Model of dynorphin-induced OPC differentiation and subsequent myelination of axons of non-dynorphin expressing neurons. During development and forced swim stress, small axonal diameter dynorphin-expressing neurons release dynorphin. Dynorphin binds KORs on OPCs causing OPCs to differentiate into myelinating oligodendrocytes, which myelinate the axons of non-dynorphin-expressing neurons.

promote OPC differentiation and myelination (Bacmeister et al., 2020; Hughes et al., 2018; McKenzie et al., 2014; Pan et al., 2020; Steadman et al., 2020; Swire et al., 2019; Xiao et al., 2016), but until now, no signal has been found to underlie this process. The discovery of neuronal glutamatergic and GABAergic synaptic input onto OPCs two decades ago (Bergles et al., 2000; Lin and Bergles, 2003) provided a compelling avenue: neurons could convey changes in experience by altering their synaptic input onto OPCs to induce OPC differentiation. Consequently, much of the focus to date has been on how these neurotransmitters act on OPCs through their ionotropic receptors. Our study, which identifies a neuropeptide as the neuronal signal underlying experience-dependent OPC differentiation and myelination following acute stress (**Figure 2.2** and **Figure 2.3**), suggests a broader approach is necessary. Dynorphin may play a similar role in

promoting OPC differentiation and myelination in other experiences involving dynorphin release, such as other stressors, during the development of neuropathic pain, and following repeated drug exposure (Knoll and Carlezon, 2010). However, dynorphin is likely only one of several signals mediating the myriad of responses of oligodendrocyte lineage cells to different experiences. Beyond promoting OPC differentiation and myelination, experience can also alter OPC proliferation (McKenzie et al., 2014; Pan et al., 2020; Steadman et al., 2020), myelin thickness (Liu et al., 2012; Makinodan et al., 2012), oligodendrocyte complexity (Makinodan et al., 2012; Swire et al., 2019), node and internode structure (Cullen et al., 2021; Etxeberria et al., 2016; Yang et al., 2020) and new internode formation (Bacmeister et al., 2020). We propose that investigation into other signals regulating these processes should consider molecules beyond the classical fast-acting neurotransmitters.

Neuropeptides and neurotrophins are attractive candidates for regulating experience-dependent plasticity in the oligodendrocyte lineage. They bind G-protein coupled receptors (GPCRs) – like kappa opioid receptor – and receptor tyrosine kinases (RTKs), respectively, providing great opportunity to affect the intracellular signaling and gene expression machinery involved in experience-dependent myelination. Indeed, several ligands of GPCRs and RTKs can mediate OPC proliferation and differentiation (Bergles and Richardson, 2016) and these receptors are upstream of the ERK/MAPK and PI3K/Akt/mTOR signaling cascades that control myelin thickness (Goebbels et al., 2010; Jeffries et al., 2016) and other pathways regulating oligodendrocyte complexity (Czopka et al., 2013; Swire et al., 2019). Furthermore, neuropeptides and neurotrophins are stored in large dense-core vesicles and released in response to high levels of neuronal activity,

providing a means by which neurons could signal changes in experience to oligodendrocyte lineage cells. A recent study found that the effects on oligodendrocyte lineage cells induced by optogenetic stimulation of layer V pyramidal neurons were dependent on BDNF (Geraghty et al., 2019), a neurotrophin that binds the RTK TrkB. Might BDNF promote experience-dependent myelination in certain learning and memory tasks where BDNF signaling is known to be engaged (Bekinschtein et al., 2014)? It should be noted, however, that direct activity-dependent release from neurons is not a necessary feature for candidate ligands if their expression or release is modulated by experience through other means. Two other studies have implicated neuregulin 1 type III and endothelin-1 and/or 3 in the deficits in oligodendrocyte complexity and social behavior observed in socially isolated mice. The mRNA for these ligands decreased following social isolation and disruption of their respective receptors, ErbB3 (an RTK) in oligodendrocytes or endothelin receptor EDNRB (a GPCR) in OPCs, phenocopied the social isolation-induced deficits in oligodendrocyte complexity and social behavior (Makinodan et al., 2012; Swire et al., 2019). We anticipate that future studies into these and other GPCR and RTK ligands will uncover many more signals regulating experience-dependent myelination.

While a role for extrinsic neuronal signaling regulating OPC differentiation and myelination in adulthood is now well accepted, the extent of its contribution to developmental myelination has been debated. Several studies have prompted the consideration that factors intrinsic to oligodendrocyte lineage cells contribute to setting up the initial myelin landscape that emerges in development. For example, OPCs are induced to differentiate once they reach a critical density *in vitro*, a phenomenon which is

dependent on the geometric and spatial constraints generated (Rosenberg et al., 2008), and oligodendrocytes do not require any axonal signaling beyond a sufficiently large diameter to form compact myelin (Lee et al., 2012). Recently, we found that in the developing optic nerve, dynamic neuronal signaling is not required for normal OPC differentiation (Mayoral et al., 2018). Although this study does not preclude a role for other non-neuronal cells in OPC differentiation, it may suggest an important role for intrinsic signaling in developmental OPC differentiation in fully myelinated white matter tracts like the optic nerve. On the other hand, studies in zebrafish larvae following the manipulation of neuronal vesicular release clearly demonstrate that extrinsic neuronal signaling can regulate spinal cord myelination in even the earliest stages of development (Hines et al., 2015; Koudelka et al., 2016; Mensch et al., 2015). Other studies in mice have shown a role for neuronal signaling in promoting OPC differentiation and myelination in the brain within the first month of life (Barak et al., 2019; Mitew et al., 2018). Evidently, more work is needed to define the relative contributions of intrinsic and extrinsic signaling to developmental OPC differentiation and myelination throughout the CNS. Here, we contribute to this debate by demonstrating that dynorphin plays a substantial role in promoting OPC differentiation and myelination at the earliest stages of myelination in the brain (**Figure 2.4 A-E**).

Timely myelination of the appropriate axons to facilitate learning and memory or otherwise advantage an organism requires the precise coordination of signals regulating new oligodendrocyte formation and the selection of which axons they will myelinate during their typically short period of myelin formation following differentiation (Bacmeister et al., 2020; Czopka et al., 2013). The appeal of neuronal control of OPC differentiation and

axon selection is that it dramatically simplifies this problem of coordination – the axons that require additional myelination could both promote OPC differentiation and their own subsequent myelination, perhaps even using the same molecular signal to regulate both processes. Considering this, we were somewhat surprised to discover that the axons of dynorphin-expressing neurons are overwhelmingly unmyelinated (**Figure 2.9** A-F and **Figure 2.10**). These findings instead support a model wherein dynorphin release from unmyelinated, dynorphin-expressing neurons acts as a diffuse OPC differentiation signal to promote the myelination of neighboring axons, which are selected for myelination through alternate means (**Figure 2.12**). How, then, in instances where the myelin demand of certain axons increases in response to experience, could dynorphin-expressing neurons coordinate dynorphin release with the presence of axon selection cues in these axons? One possibility is through shared input to both neurons. For example, in cortical layer II/III, unmyelinated dynorphin-expressing pyramidal neurons are interspersed with myelinated non-dynorphin-expressing pyramidal neurons (**Figure 2.5** I, J) whose myelination is promoted by layer II/III pyramidal neuron activity (Mitew et al., 2018). Shared inputs to activate these dynorphin- and non-dynorphin-expressing populations could coordinate the release of dynorphin to promote OPC differentiation and the expression of an axon selection cue in adjacent non-dynorphin-expressing axons to promote their selection for myelination.

Our observation that the axons of dynorphin-expressing neurons are almost entirely unmyelinated (**Figure 2.9** A-F and **Figure 2.10**) raises two other important questions. First, considering this complication of coordination, why would axons not destined for myelination regulate the myelination process? One reason might be to

preserve the ability of dynorphin-expressing neurons to promote OPC differentiation and myelination over time. Myelin coverage could obstruct axonal dynorphin release sites, so a system wherein dynorphin-expressing axons remain unmyelinated would retain its ability to promote OPC differentiation and myelination in response to stress or other experiences throughout life.

Second, how do dynorphin neurons prevent the myelination of their axons? Here, we demonstrate that their small axonal diameter is a contributing factor, but does not fully explain their lack of myelination (**Figure 2.11**). Likely, axons of dynorphin-expressing neurons are equipped with molecular factors that negatively regulate their myelination and/or they lack factors to positively promote their myelination. Might dynorphin itself act as such a negative axon selection cue? Consistent with this hypothesis, in addition to its axonal release, dynorphin is also frequently released from dendrites (Drake et al., 1994; Simmons et al., 1995; Yakovleva et al., 2006) – another structure not targeted for myelination. However, dynorphin appears to be a poor candidate to either negatively or positively regulate the selection of structures for myelination. Such cues should be precisely localized to the structure of interest. This can be readily achieved by membrane-bound adhesion molecules or through neurotransmitter release at axon-OPC synapses (Osso and Chan, 2017 or **Chapter 1**). By contrast, dynorphin's release has poor spatial resolution; unlike with classical neurotransmitters, it is often released extrasynaptically from axons (Drake et al., 1994) and there are no specialized reuptake channels localized to these sites to prevent its diffusion. More likely, dynorphin-expressing neurons use other currently undefined cues to prevent their myelination. Ultimately, the objective is to understand how such negative and positive axon selection cues coordinate with

differentiation signals like dynorphin to promote the myelination of specific axons during experience-dependent myelination, and to elucidate how this process alters behavioral outcomes.

2.5 Materials and methods

Mice

All mice were handled in accordance with the approval of the University of California, San Francisco Administrative Panel on Laboratory Animal Care and group housed under standard barrier conditions in the Laboratory Animal Research Center (LARC) in the Sandler Neurosciences Center at UCSF, Mission Bay. Mice were given food and water ad libitum and were on a 12 h light/dark cycle. Both females and males were used for all experimental conditions. *Cspg4*-CreERTM BAC transgenic mice (Zhu et al., 2011) were generously provided by Dr. Anders Persson (University of California, San Francisco; also available from Jackson Laboratory, Stock No. 008538). *Mapt*-mGFP knock-in mice (Hippenmeyer et al., 2005) were generously provided by Dr. John Rubenstein (University of California, San Francisco; also available from Jackson Laboratory, Stock No. 021162). For forced swim stress experiments, these lines were crossed to generate *Cspg4*-CreERTM/+; *Mapt*-loxP-STOP-loxP-mGFP/loxP-STOP-loxP-mGFP mice. 12-16 week old littermates of the same genotype underwent forced swim stress or served as controls. To demonstrate the suitability of this line to assess new OPC differentiation, *Cspg4*-CreERTM/+; *Mapt*-loxP-STOP-loxP-mGFP/loxP-STOP-loxP-mGFP mice and *Mapt*-loxP-STOP-loxP-mGFP/loxP-STOP-loxP-mGFP littermates were given tamoxifen or oil at postnatal day (P) 8 and analyzed at P15. *Pdyn* knock-out mice (Sharifi et al., 2001) were

generously provided by Dr. Michael Bruchas (University of Washington; also available from Jackson Laboratory, Stock No. 004272) as homozygotes. For forced swim stress experiments in *Pdyn* KO mice, *Pdyn* KO mice were crossed into *Cspg4-CreERTM* and *Mapt-mGFP* mice to generate *Cspg4-CreERTM/+*; *Mapt-loxP-STOP-loxP-mGFP/loxP-STOP-loxP-mGFP*; *Pdyn -/-* mice. 12-16 week old littermates of the same genotype underwent forced swim stress or served as controls. To compare developmental OPC differentiation and myelination, *Pdyn* KO mice were crossed with wild-type C57BL/6J mice (Jackson Laboratory, Stock No: 000664) to generate *Pdyn +/-* mice for breeding to generate *Pdyn -/-* and *Pdyn +/+* littermates, which were analyzed for developmental myelination at P8. KOR floxed (*Oprk1-loxP*) mice (Chefer et al., 2013) were generated and generously provided by Dr. Jennifer Whistler (University of California, Davis). *Olig2-Cre* mice (Schüller et al., 2008) were generously provided by Dr. David Rowitch (University of California, San Francisco; also available from Jackson Laboratory, Stock No. 011103). They were crossed with *Pdyn* KO mice to generate *Pdyn +/-*; *Olig2-Cre/+*; *Oprk1-loxP/loxP* mice and *Pdyn +/-*; *Oprk1-loxP/loxP* mice for breeding to generate *Pdyn -/-*; *Olig2-Cre/+*; *Oprk1-loxP/loxP* mice and *Pdyn +/+*; *Olig2-Cre/+*; *Oprk1-loxP/loxP* littermates for developmental myelination analysis at P8. *Pdyn-Cre* knock-in mice (Krashes et al., 2014) (Stock No. 027958) and mTmG mice (Muzumdar et al., 2007) (Stock No. 007676) were obtained from Jackson Laboratory as homozygotes. nTnG mice (Prigge et al., 2013) were generously provided by Dr. Samuel Pleasure (University of California, San Francisco; also available from Jackson Laboratory, Stock No. 023537) as homozygotes. *Pdyn-Cre* mice were bred to nTnG mice and mTmG mice to generate *Pdyn-IRES-Cre/+*; *Rosa26-loxP-ntdTomato-loxP-nEGFP/+* mice and *Pdyn-IRES-Cre/+*;

Rosa26-loxP-mtdTomato-loxP-mEGFP/+, which were analyzed for reporter expression at 12-16 weeks. STARS reporter mice (Ibrahim et al., 2018) were generated and generously provided by Dr. Li Zhang (University of Southern California; also available from Jackson Laboratory, Stock No. 032453) as heterozygous animals. They were crossed with wild-type C57BL/6J mice (Jackson Laboratory, Stock No: 000664) to establish a colony. They were then bred to *Pdyn*-Cre mice to generate *Pdyn-IRES-Cre*/+; Rosa26-lox3172-mCherry-loxP-lox3172-mEYFP-loxP/+ mice, which were analyzed for mEYFP+ axon myelination and diameters at 12-16 weeks. Details of mouse lines can be found in the **Table 2.1**. Genotypes were determined by PCR amplification and visualization with 0.0005 % ethidium bromide (BioRad, Cat. No. 161-0433) on a 2% agarose (Fisher Scientific, Cat. No. BP160-100, in 1X TAE, Fisher Scientific, Cat. No. 50-103-5139) gel. Primers and amplified fragment sizes are listed in **Table 2.2**.

Table 2.1: Key resources

Reagent or resource	Source	Identifier
Antibodies		
Rat monoclonal anti-myelin basic protein (MBP), 1:600	EMD Millipore	Cat # MAB386, RRID:AB_94975
Rabbit monoclonal anti-GFP, 1:500	Thermo Fisher Scientific	Cat # G10362, RRID:AB_2536526
Chicken polyclonal anti-GFP, 1:1000	Rockland Immunochemicals	Cat # 600-901-215, RRID:AB_1537402
Rabbit polyclonal anti-Olig2, 1:1000	EMD Millipore	Cat # AB9610, RRID:AB_570666
Mouse monoclonal CC1, 1:500	EMD Millipore	Cat # OP80, RRID:AB_2057371
Rabbit polyclonal anti-Cux1, 1:200	Santa Cruz Biotechnology	Cat # sc-13024, RRID:AB_2261231
Rat monoclonal anti-Ctip2, 1:500	Abcam	Cat # ab18465, RRID:AB_2064130
Mouse monoclonal anti-CamKIIa, 1:50	Santa Cruz Biotechnology	Cat # sc-13141, RRID:AB_626789

Reagent or resource	Source	Identifier
Antibodies		
Rabbit polyclonal anti-somatostatin (SST), 1:500	Santa Cruz Biotechnology	Cat # T-4103, RRID:AB_518614
Mouse monoclonal anti-reelin, 1:1000	EMD Millipore	Cat # MAB5364, RRID:AB_2179313
Mouse monoclonal anti-calbindin, 1:500	Swant	Cat # 300, RRID:AB_10000347
Mouse monoclonal anti-calretinin, 1:500	EMD Millipore	Cat # MAB1568, RRID:AB_94259
Rabbit monoclonal anti-neuropeptide Y (NPY), 1:1000	Cell Signaling Technology	Cat # 11976, RRID:AB_2716286
Rabbit polyclonal anti-parvalbumin (PV), 1:500	Swant	Cat # PV 27, RRID:AB_2631173
Rat monoclonal anti-CD140a/ PDGFR α , 1:500	BD Biosciences	Cat # 558774, RRID:AB_397117
Rabbit polyclonal anti-aspartoacylase (ASPA), 1:500	EMD Millipore	Cat # ABN1698, RRID:AB_2827931
Goat polyclonal anti-Sox9, 1:100	R&D Systems	Cat # AF3075, RRID:AB_2194160
Rabbit polyclonal anti-Iba1, 1:1000	Wako	Cat # 019-19741, RRID:AB_839504
Goat anti-rabbit AlexaFluor 488, 1:1000	Thermo Fisher Scientific	Cat # A-11034, RRID:AB_2576217
Donkey anti-rabbit AlexaFluor 488, 1:1000	Thermo Fisher Scientific	Cat # A-21206, RRID:AB_2535792
Goat anti-rabbit AlexaFluor 647, 1:1000	Thermo Fisher Scientific	Cat # A-21245, RRID:AB_2535813
Goat anti-rat AlexaFluor 594, 1:1000	Thermo Fisher Scientific	Cat # A-11007, RRID:AB_10561522
Goat anti-rat AlexaFluor 594, 1:800	Jackson ImmunoResearch	Cat # 112-585-167, RRID:AB_2338383
Goat anti-rat AlexaFluor 647, 1:1000	Thermo Fisher Scientific	Cat # A-21247, RRID:AB_141778
Goat anti-mouse AlexaFluor 488, 1:800	Jackson ImmunoResearch	Cat # 115-545-166, RRID:AB_2338852
Goat anti-mouse AlexaFluor 647, 1:1000	Thermo Fisher Scientific	Cat # A-21236, RRID:AB_2535805
Goat anti-chicken AlexaFluor 488, 1:1000	Thermo Fisher Scientific	Cat # A-11039, RRID:AB_142924
Donkey anti-goat AlexaFluor 647, 1:1000	Thermo Fisher Scientific	Cat # A-21447, RRID:AB_141844
Chemicals		
DAPI	Thermo Fisher Scientific	Cat # D1306

Reagent or resource	Source	Identifier
Chemicals		
Normal goat serum (NGS)	Sigma-Aldrich	Cat # G9023
Normal donkey serum (NDS)	Sigma-Aldrich	Cat # D9663
Triton X-100	Sigma-Aldrich	Cat # T8787
L.A.B. Solution	Polysciences	Cat # 24310-500
Tamoxifen	Sigma-Aldrich	Cat # T5648
nor-Binaltorphimine dihydrochloride (nor-BNI)	Sigma-Aldrich	Cat # N1771
Sodium azide	BioExpress	Cat # 0639
Paraformaldehyde (PFA)	Electron Microscopy Sciences	Cat # 19210
Mouse lines		
Mouse: <i>Cspg4</i> -CreER TM : B6.Cg-Tg(<i>Cspg4</i> - <i>cre</i> / <i>Esr1</i> *)BAKik/J	Zhu et al., 2011	RRID:IMSR_JAX:008538
Mouse: <i>Mapt</i> -mGFP: B6;129P2- <i>Mapttm2Arbrl</i> J	Hippenmeyer et al., 2005	RRID:IMSR_JAX:021162
Mouse: <i>Pdyn</i> KO: B6.129S4-Pdyntm1Ute/J	Sharifi et al., 2001	RRID:IMSR_JAX:004272
Mouse: <i>Olig2</i> -Cre: STOCK <i>Olig2^{tm2(TVA,cre)Rth}</i> J	Schüller et al., 2008	RRID:IMSR_JAX:011103
Mouse: <i>Oprk1</i> -loxP: B6-Kor tm2Jlw/Ntac	Chefer et al., 2013	N/A
Mouse: <i>Pdyn</i> -Cre: B6;129S-Pdyntm1.1(<i>cre</i>)Mjkr/LowJ	Krashes et al., 2014	RRID:IMSR_JAX:027958
Mouse: nTnG: B6N.129S6-Gt(<i>ROSA</i>)26Sortm1(<i>CAG</i> -tdTomato*, -EGFP*)Ees/J	Prigge et al., 2013	RRID:IMSR_JAX:023537
Mouse: mTmG: B6.129(Cg)-Gt(<i>ROSA</i>)26Sortm4(<i>ACTB</i> -tdTomato, -EGFP)Luo/J	Muzumdar et al. 2007	RRID:IMSR_JAX:007676
Mouse: STARS: STOCK Gt(<i>ROSA</i>)26Sortm1(<i>CAG</i> -mCherry, -EYFP*)Liiz/J	Ibrahim et al., 2018	RRID:IMSR_JAX:032453
Software		
Fiji	NIH	RRID:SCR_002285
Imaris 9.3.0	Bitplane	RRID:SCR_007370
GraphPad Prism 7	GraphPad	RRID:SCR_002798
Adobe Illustrator CC 2017	Adobe	RRID:SCR_010279
Microscopes		
Zeiss Axio Scan Z1 Slide Scanner	Zeiss	N/A
Zeiss LSM 700 laser scanning confocal microscope	Zeiss	N/A
Zeiss Axio Imager M2 microscope	Zeiss	N/A

Table 2.2: Genotyping primers and amplified fragment sizes

Reagent or resource	Source	Identifier
Primers		
<i>Cspg4</i> -CreER TM : Wildtype: GAT GTG AAT AAA AGG CGA CAT TC (261bp), Mutant: CTG AAC GGG CAG ATC AAC AT (220bp), Common: TGT ATT ATT TTC CAT ACT AGA TGT CCA	Jackson Laboratory	37524, 37525, 37536
<i>Mapt</i> -mGFP: Wild-type: TGT GTA TGT CCA CCC CAC TG (224bp), Mutant: AAA CAT GTC CCA GCT CCA AG (280bp), Common: CCT TGT CCC CAA CTC CAT AC	Jackson Laboratory	17461, 17462, 17460
<i>Pdyn</i> KO: Wild-type: CCA TGA GGA ACT GCA TCG GA (332bp), Mutant: GGC TAC CCG TGA TAT TGC TGA (669bp), Common: TAT CTG CCT GGA GAT GGG GA	This manuscript	N/A
<i>Olig2</i> -Cre: Wild-type: CAC AGG AGG GAC TGT GTC CT (392bp), Mutant: GCC AGA GGC CAC TTG TGT AG (500bp), Common: AGT TGG TGA GCA TGA GGA TG	Jackson Laboratory	12704, oIMR7415, 12705
<i>Oprk1</i> -loxP: AGG CAC AGT GGG GAA ATT GCT GTG and ACT GGG AGA GCA GGT AGG GCC TGG (Wildtype: 424bp, Mutant: 558bp); Floxed out: CCT GCA GGA AGT ACC AGA GC (339bp) used in the same reaction with the common primers to detect germline recombination	Dr. Jennifer Whistler; this manuscript	N/A
<i>Pdyn</i> -Cre: Wild-type: GCT CAT TTT TCT TCC GAG AGG (425bp), Mutant: ACA CCG GCC TTA TTC CAA G (110bp), Common: CCA GGA GAA CCC CAA TAC CT	Jackson Laboratory	25683, 13007, 25682
nTnG: Wild-type: CTT TAA GCC TGC CCA GAA GA (252bp), Mutant: GGG CGT ACT TGG CAT ATG AT (495bp), Common: GCA CTT GCT CTC CCA AAG TC	Martinez et al., 2019	N/A
mTmG: Wild-type: AGG GAG CTG CAG TGG AGT AG (212bp), Mutant: TAG AGC TTG CGG AAC CCT TC (128bp), Common: CTT TAA GCC TGC CCA GAA GA	Jackson Laboratory	30298, 30297, 12177
STARS: Wild-type: AAG GGA GCT GCA GTG GAG TA and CCG AAA ATC TGT GGG AAG TC (297bp); Mutant: GCC TCT GCT AAC CAT GTT CAT GCC TTC TTC and CTT GAA GCG CAT GAA CTC CTT GAT GAT G (219bp).	Jackson Laboratory; Ibrahim et al., 2018	oIMR9020, oIMR9021; N/A

Forced swim stress

Forced swim stress was performed in 12-16 week old mice as previously described (McLaughlin et al., 2003). Both experimental mice and controls were brought in their home cage to the behavior room 1 h prior to swim. Experimental mice were placed in an opaque 5 gallon (28.5 cm diameter, 37 cm tall) bucket filled to a depth of 20 cm with 30 °C tap water to swim without the opportunity to escape. After each trial, mice were dried with paper towel and returned to their home cage. Control mice remained in the home cage. On the first day, experimental mice swam for a single trial of 15 min. On the second day, experimental mice swam for four trials of 6 min each, each separated by 7 min in their home cage. All mice were returned to the mouse facility within 10 min of the final swim on both days.

Drug administration

Tamoxifen (Sigma-Aldrich, Cat. No. T5648) was stored as a powder at 4 °C protected from light. On the day of administration, tamoxifen was weighed and dissolved in peanut oil to a concentration of 1 mg/mL. The solution was shaken at 1000rpm at 42 °C for several hours until tamoxifen had dissolved. Forced swim stressed mice and littermate controls were administered 60 µL of solution by oral gavage three days prior to the first forced swim stress trial. P8 pups were administered a comparable dose for their weight (10 µL) by gavage. Nor-Binaltorphimine dihydrochloride (nor-BNI, Sigma-Aldrich, Cat. No. N1771) was stored as a powder at -20 °C. On the day of administration, nor-BNI was weighed and dissolved in autoclaved phosphate buffered saline (PBS, in Milli-Q Synthesis A10 purified water, pH 7.4) to a concentration of 1 mg/mL. The solution was shaken at

1000rpm at room temperature (RT) for 20 min until nor-BNI had dissolved, and then filtered through a 0.22 μm filter (EMD Millipore, Cat. No. SLGP033RS). As previously described, the solution was administered by intraperitoneal injection at 10 mg/kg to both experimental and control animals 1 h prior to the first swim trial on both days of forced swim stress sessions (McLaughlin et al., 2003).

Tissue processing and immunohistochemistry

Mice were deeply anesthetized with intraperitoneal injection of 2,2,2-tribromoethyl alcohol (Sigma-Aldrich, Cat. No. T48402) and perfused transcardially with 1X PBS followed by 4% paraformaldehyde (PFA, Electron Microscopy Sciences, Cat. No. 19210 in PBS, pH 7.4). Brains were immediately dissected from the skull and post-fixed in 4% PFA at 4 °C for 2 h (for immunostaining for ASPA, CD140a, PV, calretinin, and calbindin, as well as GFP when used in the same sections) or overnight (all other immunostaining). Brains were rinsed with 1X PBS + 0.02% sodium azide (BioExpress, Cat. No. 0639) and transferred to 30% sucrose (Sigma-Aldrich, Cat. No. S9378) + 0.02% sodium azide (in PBS) solution for cryoprotection until sinking (~48 h at 4 °C). Brains were mounted with a 2:1 30% sucrose:optimum cutting temperature solution (OCT, Tissue-Tek, Cat. No. 4583) to a freezing stage (Thermo Fisher Scientific, KS 34) and cryosectioned using a sliding microtome (Thermo Fisher Scientific, HM 450) coronally at 30 μm thickness. Sections for CamKIIa immunostaining were 14 μm to allow for penetration of the CamKIIa antibody through the entire tissue. Sections for analysis of mEYFP+ axon myelination and diameters were 6 μm to allow for penetration of the MBP antibody into dense white matter tracts. Floating sections were stored in 1X PBS + 0.02% sodium azide at 4 °C until

immunostaining. For immunostaining, floating sections were blocked and permeabilized in 20% normal goat serum (NGS, Sigma-Aldrich, Cat. No. G9023) + 0.2% Triton X-100 (Sigma-Aldrich, Cat. No. T8787, in DPBS with calcium, magnesium, Thermo Fisher Scientific, Cat. No. 14040133) for 2 h shaking at 80 rpm at RT. Sections were then incubated in primary antibodies diluted in fresh blocking solution overnight (two overnights for CamKIIa immunostaining) shaking at 55 rpm at 4 °C. Primary antibodies and their dilutions are listed in the **Table 2.1**. Sections were washed in PBS for 30 min shaking at 80 rpm at RT and then incubated in secondary antibodies diluted in 20% NGS for 1 h shaking at 80 rpm at RT. Secondary antibodies and their dilutions were as follows: AlexaFluor 488-, AlexaFluor 594-, and AlexaFluor 647-conjugated goat antibodies to rat, rabbit, mouse, and chicken (1:1000, Thermo Fisher Scientific, Cat. Nos. A-21245, A-11034, A-11007, A-21236, A-21247, A-11039). To prevent cross-reaction when rat and mouse primary antibodies were used in the same sections, secondary antibodies from Jackson ImmunoResearch were used (1:800, Cat. Nos. 115-545-166, 112-585-167). For sections with goat primary antibody, 10% normal donkey serum (NDS, Sigma-Aldrich, Cat. No. D9663, in DPBS with calcium, magnesium) was used in place of 20% NGS for all steps; secondary antibodies were donkey (Thermo Fisher Scientific, Cat Nos. A-21206, A-21447). DAPI (40ng/ml, Thermo Fisher Scientific, Cat No. D1306) was added for the last 8 min of secondary antibody incubation. Sections were then washed in PBS for 30min shaking at 80 rpm at RT, mounted onto Superfrost Plus microscope slides (Thermo Fisher Scientific, Cat. No. 12-550-15), dried, rinsed in water, and dried again. Slides were then coverslipped (Thermo Fisher Scientific, Cat. No. 12-543C) using Glycergel Mounting Medium (Agilent, Cat. No. C0563) for imaging. Antigen retrieval was

required for CamKIIa immunostaining. Prior to blocking, floating sections were washed in PBS and incubated for 7 min in L.A.B. Solution (Polysciences, Cat No. 24310-500) then washed again in PBS shaking at 80 rpm at RT. To adequately visualize individual myelin sheaths with MBP immunostaining in densely myelinated regions for analysis of mEYFP+ axon myelination, prior to blocking, floating sections were dipped in water, then dehydrated and rehydrated using ascending then descending ethanol (Sigma-Aldrich, Cat. No. E7023) dilutions (50, 70, 90, 95, 100, 95, 90, 70, 50% in water) for 2 min each shaking at 80 rpm at RT as previously described (Duncan et al., 2018), then dipped in water again, and finally washed in PBS until blocking.

Image acquisition

All analysis was centered around Bregma 0.9 mm. To verify the effectiveness of using *Cspg4-CreERTM*; *Mapt-mGFP* mice to identify newly differentiated oligodendrocytes, five consecutive 30 μ m coronal sections centered around Bregma 0.9mm were immunostained per pup. One hemisphere was imaged per section for a total of five images per mouse. Tiled z stack images comprising six 20X tiles in a consistent region in dorsal striatum were taken using a Zeiss LSM 700 laser scanning confocal microscope. The same imaging settings were used for all images across all experimental replicates. To compare OPC differentiation in forced swim stressed mice and controls, in each mouse, every fifth section from Bregma 1.5 mm to Bregma 0.3 mm was immunostained, for a total of eight 30 μ m coronal sections centered around Bregma 0.9mm. Tiled z stacks of each full section were taken using a Zeiss Axio Scan Z1 Slide Scanner at 20X. The same imaging settings were used for all images across all experimental replicates. For

presentation in figures to improve contrast of mGFP and MBP staining against the background and for higher magnification images, representative images were taken using a Zeiss LSM 700 laser scanning confocal microscope. To compare developmental OPC differentiation and myelination, in each mouse, five consecutive 30 μm coronal sections centered around Bregma 0.9 mm were immunostained. Immunofluorescent images were acquired on a Zeiss Axio Imager M2 with a Zeiss AxioCam MRm and Zeiss Apotome 2. The same imaging settings were used for all mice within an experimental replicate. For MBP area, 3-4 tiled 10X z stack images encompassing the entire region shown in **Figure 2.4 A, F** were taken per mouse. Only one hemisphere per section was imaged. For CC1+MBP+Olig2⁺ and Olig2⁺ cell quantification, both hemispheres were imaged if possible and a total of 7-10 tiled 10X z stack images encompassing the region shown in **Figure 2.4 C, H** were taken per mouse. For analysis of dynorphin reporter expression, consecutive 30 μm coronal sections centered around Bregma 0.9mm were immunostained for EGFP and several neuronal and glial markers. Sections immunostained for CamKII α were 14 μm (see “Tissue processing and immunohistochemistry”). For quantification of colocalization of nEGFP with each neuronal marker, two sections were imaged per mouse in each brain region using a Zeiss LSM 700 laser scanning confocal microscope. Per section, one tiled 20X z stack image encompassing all EGFP⁺ cells in the isocortex of one hemisphere, excluding the medial region, was taken. In dorsal and ventral striatum, one tiled image of four and two 20X z stack tiles was taken per section, respectively. For analysis of mEYFP⁺ axon myelination and diameters, consecutive 6 μm coronal sections centered around Bregma 0.9mm were imaged using a Zeiss LSM 700 laser scanning confocal microscope. Six 63X z stack

images were taken per mouse (3 per section, 2 sections per mouse) in medial cortical layer VI, lateral cortical layer I, and distributed throughout the dorsal striatum.

Image blinding and analysis

In *Cspg4-CreERTM*; *Mapt*-mGFP pups, quantification of mGFP area was performed with Fiji software (NIH) using maximum intensity projections of z stack tiled images. Images were randomized and blinded using a Java program written by L.A.O. prior to any analysis. The entire region of each acquired image was quantified. mGFP area was measured as the area of pixels above a threshold intensity and was divided by the total area per image to get the percentage of area that was mGFP+. In each mouse, this value was averaged across all images to get an average value per mouse. In forced swim stress experiments, quantification was performed with Fiji software using stacks of 10 individual z planes to allow for unambiguous identification of the soma of mGFP+MBP+ cells (by colocalization with DAPI). Images were randomized and blinded using a Java program written by L.A.O. prior to any analysis. All mGFP+MBP+ somas were quantified in the entire isocortex and striatum (caudoputamen and nucleus accumbens) of all sections. Density per section was determined by dividing the number of mGFP+MBP+ cells by the area of the region of interest, which was manually delineated using landmarks defined by DAPI and MBP. In each mouse, this value was averaged across all sections to provide the average cell density per mouse, which was then normalized to the control average per cohort. To analyze developmental OPC differentiation and myelination, maximum intensity projections of z stacks were analyzed using Fiji software. Images were randomized and blinded using a Java program written by L.A.O. prior to any analysis.

Regions for analysis were standardized using the same ROI for all images, which was positioned based on brain landmarks defined by DAPI. MBP area was measured as the area of pixels above a threshold intensity. Quantification of cell density was performed manually. In each mouse, quantification from all images was averaged, and that average was then normalized to the control average per litter. For quantification of colocalization of dynorphin-expressing EGFP+ nuclei with neuronal markers, maximum intensity projections of z stacks were analyzed using either Fiji or Imaris 9.3.0 software (Bitplane). Using Fiji, quantification was performed manually. Using Imaris, quantification was performed using the Surfaces tool and verified manually. All EGFP+ nuclei within the imaged regions were quantified. The delineation between upper and deeper cortical layer cells was performed based on localization in the cortex using the EGFP+ channel and DAPI without looking at colocalization with neuronal markers. Quantification of mEYFP+ axon myelination was performed with Fiji using a stack of the maximum intensity z projection and each individual z plane for an image. mEYFP+ segments were traced with the Freehand Line tool and added to the ROI Manager. Panning through individual z planes allowed for accurate tracing of overlapping mEYFP+ segments. To determine if mEYFP+ segments were myelinated, colocalization with MBP immunostaining was examined across z planes. To compare mEYFP+ segment myelination in control and forced swim stressed mice, images were first randomized and blinded using a Java program written by L.A.O. prior to any analysis. Quantification of mEYFP+ axon diameter was performed on half of the images used for percentage myelination quantification (three 63X confocal images per region per mouse). Maximum intensity z projection images with annotated unmyelinated and myelinated axons were opened in Fiji. The mEYFP fluorescent intensity

was averaged across a 1 μm length of axon by drawing a line (with 1 μm thickness) transecting the axon in a representative linear region and using the “Plot Profile” tool. Only axons with linear regions $\geq 1 \mu\text{m}$ unobstructed by other mEYFP axons were used. Then, a Gaussian curve was fit to the distribution. Axons were only included if $R^2 > 0.90$. The full width at half maximum (FWHM) was calculated from the standard deviation of the Gaussian curve and used as the estimate for that axon’s diameter. With these parameters, we were able to quantify the diameters of 39.62% of mEYFP+ axons in cortical layer VI, 45.34% in cortical layer I, 47.69% in striatal GM, and 55.32% in striatal WM of the images analyzed.

Statistical analysis

Statistical analysis and graphing were performed with Prism 7 software (GraphPad). Statistical comparisons in **Figure 2.2**, **Figure 2.3**, **Figure 2.4**, and **Figure 2.9** were performed using an unpaired two-tailed Student’s t test; in **Figure 2.1** using a one-way ANOVA with Tukey’s multiple comparisons; in **Figure 2.11** using a two-tailed Mann-Whitney test. Significance was determined by * $P < 0.05$. Data distribution was assumed to be normal, except in **Figure 2.11**, where a non-parametric test was used to account for the distribution of myelinated mEYFP+ axons. N values represent the number of mice in all figures except **Figure 2.11**, where N represents the number of axons. Data are reported as mean \pm s.e.m. when a Student’s t test or a one-way ANOVA was performed on the data; descriptive data are reported as mean \pm s.d. Samples sizes and statistical details for each experiment are described in the figure legends.

CHAPTER 3: Conclusion

3.1 Synthesis

Chapter 1 of this dissertation describes the known patterns of CNS myelination and provides a framework to understand how this architecture could emerge, using it to evaluate previous work in this field. Briefly, myelination is heterogeneous between CNS regions. White matter regions have a higher density of oligodendrocytes and are more highly myelinated than gray matter regions (Dawson et al., 2003); within cortex, the same is true for deeper cortical layers over those more superficial (Hughes et al., 2018). Within a region, certain axons are more heavily myelinated than others. Which axons are selected for myelination is strongly determined by axonal diameter (Lee et al., 2012; Stedehouder et al., 2019; Sturrock, 1980) as well as by neuronal subtype (Call and Bergles, 2021; Micheva et al., 2016; Stedehouder et al., 2017).

Table 3.1: Factors regulating oligodendrocyte formation or axon selection

	Dynamic	Static
Positive	Inductive	Attractive
Negative	Preventative	Repulsive
Permissive	Dynamically Permissive	Statically Permissive

To understand how these patterns could emerge, I outline a framework to classify factors that could regulate (1) the localization of oligodendrocytes (oligodendrocyte formation) and (2) around which axons those oligodendrocytes form their myelin sheaths (axon selection). I discuss these factors primarily in the context of regulating axon

selection, but this framework applies to factors regulating oligodendrocyte formation as well. Such factors can positively or negatively regulate oligodendrocyte formation or axon selection, and can be either dynamically regulated (turning on or off) or static (**Table 3.1**). Furthermore, the environment must be permissive for oligodendrocytes and myelin (**Table 3.1**). The central question of **Chapter 1** interrogates how these signals could work together to ensure the correct localization of oligodendrocytes and myelin sheaths at any time for proper nervous system function.

In **Chapter 2**, I present my experimental work demonstrating that the neuropeptide dynorphin acts as a neuronal signal promoting OPC differentiation and myelination both during development and following acute stress. We identified several populations of neurons that express dynorphin in the brain and found that they are all overwhelming unmyelinated under normal conditions and following acute stress. Finally, we found that the lack of myelination of these axons was partially attributable to their small axonal diameters and partially attributable to their neuronal subtype. We propose the following model whereby developmental and experience-dependent myelination is mediated by small axonal diameter, unmyelinated, dynorphin-expressing neurons that release dynorphin to promote OPC differentiation for the myelination of neighboring axons.

Here, I evaluate our work from **Chapter 2** using the framework I present in **Chapter 1**. During acute stress, we can conclude that dynorphin acts as a *inductive* cue for oligodendrocyte formation (**Table 3.1**). The release of dynorphin is dynamically regulated by stress (Bruchas et al., 2008; Schindler et al., 2012) and its increased release promotes OPC differentiation. An outstanding question is whether dynorphin acts as a dynamic or static cue during development. Do specific experiences or developmental stages

dynamically regulate dynorphin release over the course of normal development? Or is dynorphin released statically, either due to baseline patterns of neuronal activity or perhaps – like with neurotrophins (Al-Qudah and Al-Dwairi, 2016) – via an activity-independent constitutive release pathway?

We observed an overwhelming lack of myelination of dynorphin-expressing neurons well into adulthood. This could occur through several different scenarios. First, it is possible that the axons of dynorphin-expressing neurons are statically non-*permissive* for myelination (**Table 3.1**). Indeed, we found that a substantial proportion of these axons were below the threshold diameter required for myelination. However, the majority of axons were suprathreshold, indicating that additional factors must also contribute to ensure the axons of dynorphin-expressing neurons remain unmyelinated.

These axons might express a (static) *repulsive* cue, preventing their myelination throughout the lifetime (**Table 3.1**). Alternatively, or additionally, these axons might lack sufficiently *attractive* or *inductive* cues to promote their myelination (**Table 3.1**). We observed that among axons of dynorphin-expressing neurons presumably *permissive* for myelination (above 0.3 μm in diameter), axonal diameter still influenced myelination status. Smaller diameter axons were less likely to be myelinated than those larger. As a continuous variable, axon diameter does not neatly fit into a categorical classification of positive or negative (**Table 3.1**), but nevertheless, we can conclude that decreasing axon diameter negatively influences axon selection while increasing axon diameter positively influences axon selection. However, we observed that even at the same axon size, dynorphin-expressing neurons were less likely to be myelinated than other CNS neuronal subtypes, indicating that factors beyond axonal diameter are involved in preventing their

myelination. It seems likely that dynorphin-expressing neurons express some non-size-related *repulsive* cues that these other subtypes lack and/or lack some non-size-related positive axon selection cues expressed by these other subtypes (**Table 3.1**).

What about the few axons of dynorphin-expressing neurons that are myelinated? Can their selection for myelination be attributed entirely to their larger axonal diameters? Or, might the myelinated and unmyelinated axons within a dynorphin-expressing subtype differ in levels of non-size-related axon selection cues? It seems both size-related and non-size-related axon selection cues likely contribute to their selection for myelination. While myelinated axons of dynorphin-expressing neurons were indeed on average larger than those that were unmyelinated, the axon diameter distributions of these two populations overlapped heavily. Furthermore, different subtypes of dynorphin-expressing neurons with almost identical axon diameter distributions (cortical layer I and striatal GM axons) had different rates of myelination. Axons of dynorphin-expressing neurons in cortical layer I were never myelinated, while those in the striatal GM were myelinated at a rate of 0.60%, suggesting that axon selection cues beyond size are likely involved in the selection of this small proportion of striatal GM axons for myelination. Future interrogation into the potential molecular differences between myelinated and unmyelinated axons within a dynorphin-expressing neuronal subtype may be a tractable approach to discovering new axon selection cues. In contrast to comparing two different neuronal subtypes with different rates of myelination, molecular comparison within a neuronal subtype avoids subtype-specific molecular differences irrelevant to selection for myelination.

Finally, our experimental work touches on the central question raised in **Chapter 1**: how signals regulating oligodendrocyte formation and axon selection temporally and

spatially coordinate to ensure correct localization of oligodendrocytes and myelin sheaths at any time for proper nervous system function. The simplest scenario proposed in **Chapter 1** – one that has gained traction in the field – is that axons requiring myelination could promote oligodendrocyte formation and their own subsequent myelination, perhaps even using the same cue to regulate both processes. Our data support a different model, wherein dynorphin-expressing neurons use an *inductive* cue (dynorphin release) to promote oligodendrocyte formation not for their own myelination, but rather for the myelination of other axons. Understanding how this *inductive* oligodendrocyte formation cue is coordinated with axon selection cues in neighboring axons to ensure the correct axons are myelinated at any time is an important future direction.

3.2 Significance

One of the most intimate interactions in the nervous system is the one formed by neurons and oligodendrocytes. Consider, for instance, that early observers thought myelin was derived from the axon itself (Boullerne, 2016). And so, as oligodendrocyte lineage cells were increasingly understood to be regulated by extrinsic factors, neurons emerged as the candidate source of these signals. Since the earliest studies testing this hypothesis three decades ago (Barres and Raff, 1993; Barres et al., 1993), we have accumulated substantial evidence supporting a role for neurons in regulating oligodendrocyte lineage cells (Gibson et al., 2014; Mitew et al., 2018; Barak et al., 2019). Furthermore, we have found evidence that this cell lineage responds to experience and that this response is important for learning and memory (Bacmeister et al., 2020; Cullen et al., 2021; Etxeberria et al., 2016; Hughes et al., 2018; Liu et al., 2012; Makinodan et al., 2012; McKenzie et

al., 2014; Pan et al., 2020; Steadman et al., 2020; Swire et al., 2019; Wang et al., 2020; Xiao et al., 2016; Xin and Chan, 2020; Yang et al., 2020). Along with work in other non-neuronal CNS cell types, these studies have helped to dramatically expand our understanding of the functions of glia beyond “glue”.

The gap in this field has been in understanding precisely how neurons or experiences regulate oligodendrocyte lineage cells. Our work has provided the first description (to our knowledge) of a molecular signal underlying experience-dependent changes in oligodendrocyte lineage cells. Although it had been widely hypothesized that glutamate or GABA release at neuron-OPC synapses was likely to underlie experience-dependent myelination, here we show that a neuropeptide mediates this process. I expect this work will be followed by the discovery of numerous other mechanisms underlying experience-dependent changes in oligodendrocyte lineage cells in different behaviors and brain regions. I hope our findings inspire the investigation into other neuropeptides and molecules beyond the classical neurotransmitters in this search.

Second, our findings establish the novel concept of unmyelinated neurons regulating the myelination process. This challenges the historical perception of neurons as the logical mediators of this process due to their own targeting for myelination and introduces new intermediate cellular players. I hope that our results instigate a broader consideration of unmyelinated cells – neuronal and otherwise – as regulators of myelination developmentally and in response to experience.

3.3 Reflections

This dissertation encompasses six years of work that I began in 2015 in the laboratory of

Jonah Chan at UCSF. It has been an honor and a privilege to work on this project and I have been deeply humbled by the challenge. I hope that the data and ideas presented here can help guide us toward a better understanding of CNS myelination and an appreciation of its intricate and wondrous nature.

REFERENCES

Almeida, R., and Lyons, D. (2016). Oligodendrocyte Development in the Absence of Their Target Axons In Vivo. *PLoS One* 11, e0164432.

Almeida, R.G., Czopka, T., French-Constant, C., and Lyons, D.A. (2011). Individual axons regulate the myelinating potential of single oligodendrocytes in vivo. *Development* 138, 4443–4450.

Almeida, R.G., and Lyons, D.A. (2014). On the resemblance of synapse formation and CNS myelination. *Neuroscience* 276, 98–108.

Al-Qudah, M.A., and Al-Dwairi, A. (2016). Mechanisms and regulation of neurotrophin synthesis and secretion. *Neurosciences* 21, 306–313.

Bacmeister, C.M., Barr, H.J., McClain, C.R., Thornton, M.A., Nettles, D., Welle, C.G., and Hughes, E.G. (2020). Motor learning promotes remyelination via new and surviving oligodendrocytes. *Nat. Neurosci.* 23, 819–831.

Barak, B., Zhang, Z., Liu, Y., Nir, A., Trangle, S.S., Ennis, M., Levandowski, K.M., Wang, D., Quast, K., Boulting, G.L., et al. (2019). Neuronal deletion of *Gdf2i*, associated with Williams syndrome, causes behavioral and myelin alterations rescuable by a remyelinating drug. *Nat. Neurosci.* 22, 700–708.

Barres, B.A., Hart, I.K., Coles, H.S., Burne, J.F., Voyvodic, J.T., Richardson, W.D., and Raff, M.C. (1992). Cell death and control of cell survival in the oligodendrocyte lineage. *Cell* 70, 31–46.

Barres, B.A., Jacobson, M.D., Schmid, R., Sendtner, M., and Raff, M.C. (1993). Does oligodendrocyte survival depend on axons? *Curr. Biol.* 3, 489–497.

Barres, B.A., and Raff, M.C. (1993). Proliferation of oligodendrocyte precursor cells depends on electrical activity in axons. *Nature* 361, 258–260.

Bechler, M.E., Byrne, L., and French-Constant, C. (2015). CNS Myelin Sheath Lengths Are an Intrinsic Property of Oligodendrocytes. *Curr. Biol.* 25, 2411–2416.

Bekinschtein, P., Cammarota, M., and Medina, J.H. (2014). BDNF and memory processing. *Neuropharmacology* 76, 677–683.

Bergles, D.E., and Richardson, W.D. (2016). Oligodendrocyte Development and Plasticity. *Cold Spring Harb. Perspect. Biol.* 8, a020453.

Bergles, D.E., Roberts, D.J., Somogyi, P., and Jahr, C.E. (2000). Glutamatergic synapses on oligodendrocyte precursor cells in the hippocampus. *Nature* 405, 187–191.

Biase, L.M.D., Nishiyama, A., and Bergles, D.E. (2010). Excitability and synaptic communication within the oligodendrocyte lineage. *J. Neurosci.* 30, 3600–3611.

Bishop, G.H., Clare, M.H., and Landau, W.M. (1971). The relation of axon sheath thickness to fiber size in the central nervous system of vertebrates. *Int. J. Neurosci.* 2, 69–77.

Boullerne, A.I. (2016). The history of myelin. *Exp. Neurol.* 283, 431–445.

Bridges, A.A., Jentsch, M.S., Oakes, P.W., Occhipinti, P., and Gladfelter, A.S. (2016). Micron-scale plasma membrane curvature is recognized by the septin cytoskeleton. *J. Cell Biol.* 213, 23–32.

Brinkmann, B.G., Agarwal, A., Sereda, M.W., Garratt, A.N., Müller, T., Wende, H., Stassart, R.M., Nawaz, S., Humml, C., Velanac, V., et al. (2008). Neuregulin-1/ErbB signaling serves distinct functions in myelination of the peripheral and central nervous system. *Neuron* 59, 581–595.

Bruchas, M.R., Xu, M., and Chavkin, C. (2008). Repeated swim stress induces kappa opioid-mediated activation of extracellular signal-regulated kinase 1/2. *Neuroreport* 19, 1417–1422.

Call, C.L., and Bergles, D.E. (2021). Remyelination restores myelin content on distinct neuronal subtypes in the cerebral cortex. *bioRxiv* 2021.02.17.431685.

Calver, A.R., Hall, A.C., Yu, W.-P., Walsh, F.S., Heath, J.K., Betsholtz, C., and Richardson, W.D. (1998). Oligodendrocyte Population Dynamics and the Role of PDGF In Vivo. *Neuron* 20, 869–882.

Charles, P., Hernandez, M.P., Stankoff, B., Aigrot, M.S., Colin, C., Rougon, G., Zalc, B., and Lubetzki, C. (2000). Negative regulation of central nervous system myelination by polysialylated-neural cell adhesion molecule. *Proc. Natl. Acad. Sci. U. S. A.* 97, 7585–7590.

Cheadle, L., Rivera, S.A., Phelps, J.S., Ennis, K.A., Stevens, B., Burkly, L.C., Lee, W.-C.A., and Greenberg, M.E. (2020). Sensory Experience Engages Microglia to Shape Neural Connectivity through a Non-Phagocytic Mechanism. *Neuron* 108, 451–468.

Chefer, V.I., Bäckman, C.M., Gigante, E.D., and Shippenberg, T.S. (2013). Kappa Opioid Receptors on Dopaminergic Neurons Are Necessary for Kappa-Mediated Place Aversion. *Neuropsychopharmacology* 38, 2623–2631.

Chong, S.Y., Rosenberg, S.S., Fancy, S.P., Zhao, C., Shen, Y.-A.A., Hahn, A.T., McGee, A.W., Xu, X., Zheng, B., Zhang, L.I., et al. (2012). Neurite outgrowth inhibitor Nogo-A establishes spatial segregation and extent of oligodendrocyte myelination. *Proc. Natl. Acad. Sci. U. S. A.* 109, 1299–1304.

Cullen, C.L., Pepper, R.E., Clutterbuck, M.T., Pitman, K.A., Oorschot, V., Auderset, L., Tang, A.D., Ramm, G., Emery, B., Rodger, J., et al. (2021). Periaxonal and nodal plasticities modulate action potential conduction in the adult mouse brain. *Cell Rep.* 34, 108641.

Czopka, T., Ffrench-Constant, C., and Lyons, D.A. (2013). Individual oligodendrocytes have only a few hours in which to generate new myelin sheaths in vivo. *Dev. Cell* 25, 599–609.

Dawson, M.R.L., Polito, A., Levine, J.M., and Reynolds, R. (2003). NG2-expressing glial progenitor cells: an abundant and widespread population of cycling cells in the adult rat CNS. *Mol. Cell. Neurosci.* 24, 476–488.

Drake, C., Terman, G., Simmons, M., Milner, T., Kunkel, D., Schwartzkroin, P., and Chavkin, C. (1994). Dynorphin opioids present in dentate granule cells may function as retrograde inhibitory neurotransmitters. *J. Neurosci.* 14, 3736–3750.

Du, C., Duan, Y., Wei, W., Cai, Y., Chai, H., Lv, J., Du, X., Zhu, J., and Xie, X. (2016). Kappa opioid receptor activation alleviates experimental autoimmune encephalomyelitis and promotes oligodendrocyte-mediated remyelination. *Nat. Commun.* 7, 11120.

Duncan, G.J., Manesh, S.B., Hilton, B.J., Assinck, P., Liu, J., Moulson, A., Plemel, J.R., and Tetzlaff, W. (2018). Locomotor recovery following contusive spinal cord injury does not require oligodendrocyte remyelination. *Nat. Commun.* 9, 3066.

Etxeberria, A., Hokanson, K.C., Dao, D.Q., Mayoral, S.R., Mei, F., Redmond, S.A., Ullian, E.M., and Chan, J.R. (2016). Dynamic Modulation of Myelination in Response to Visual Stimuli Alters Optic Nerve Conduction Velocity. *J. Neurosci.* 36, 6937–6948.

Fanarraga, M., Griffiths, I., Zhao, M., and Duncan, I. (1998). Oligodendrocytes are not inherently programmed to myelinate a specific size of axon. *J. Comp. Neurol.* 399, 94–100.

Foran, D.R., and Peterson, A.C. (1992). Myelin acquisition in the central nervous system of the mouse revealed by an MBP-Lac Z transgene. *J. Neurosci.* 12, 4890–4897.

Ford, M.C., Alexandrova, O., Cossell, L., Stange-Marten, A., Sinclair, J., Kopp-Scheinflug, C., Pecka, M., Attwell, D., and Grothe, B. (2015). Tuning of Ranvier node and internode properties in myelinated axons to adjust action potential timing. *Nat. Commun.* 6, 8073.

Fu, M., and Zuo, Y. (2011). Experience-dependent structural plasticity in the cortex. *Trends Neurosci.* 34, 177–187.

Geraghty, A.C., Gibson, E.M., Ghanem, R.A., Greene, J.J., Ocampo, A., Goldstein, A.K., Ni, L., Yang, T., Marton, R.M., Paşca, S.P., et al. (2019). Loss of Adaptive Myelination Contributes to Methotrexate Chemotherapy-Related Cognitive Impairment. *Neuron* 103, 250–265.

Gerfen, C., Engber, T., Mahan, L., Susel, Z., Chase, T., Monsma, F., and Sibley, D. (1990). D1 and D2 dopamine receptor-regulated gene expression of striatonigral and striatopallidal neurons. *Science* 250, 1429–1432.

Gibson, E.M., Purger, D., Mount, C.W., Goldstein, A.K., Lin, G.L., Wood, L.S., Inema, I., Miller, S.E., Bieri, G., Zuchero, B.J., et al. (2014). Neuronal Activity Promotes Oligodendrogenesis and Adaptive Myelination in the Mammalian Brain. *Science* 344, 1252304.

Goebbels, S., Oltrogge, J.H., Kemper, R., Heilmann, I., Bormuth, I., Wolfer, S., Wichert, S.P., Möbius, W., Liu, X., Lappe-Siefke, C., et al. (2010). Elevated phosphatidylinositol 3,4,5-trisphosphate in glia triggers cell-autonomous membrane wrapping and myelination. *J. Neurosci.* 30, 8953–8964.

Goebbels, S., Wieser, G.L., Pieper, A., Spitzer, S., Weege, B., Yan, K., Edgar, J.M., Yagensky, O., Wichert, S.P., Agarwal, A., et al. (2017). A neuronal PI(3,4,5)P3-dependent program of oligodendrocyte precursor recruitment and myelination. *Nat. Neurosci.* 20, 10–15.

Harris, J.J., and Attwell, D. (2012). The energetics of CNS white matter. *J. Neurosci.* 32, 356–371.

Hill, R.A., Li, A.M., and Grutzendler, J. (2018). Lifelong cortical myelin plasticity and age-related degeneration in the live mammalian brain. *Nat. Neurosci.* 21, 683–695.

Hines, J.H., Ravanelli, A.M., Schwindt, R., Scott, E.K., and Appel, B. (2015). Neuronal activity biases axon selection for myelination in vivo. *Nat. Neurosci.* 18, 683–689.

Hippenmeyer, S., Vrieseling, E., Sigrist, M., Portmann, T., Laengle, C., Ladle, D.R., and Arber, S. (2005). A Developmental Switch in the Response of DRG Neurons to ETS Transcription Factor Signaling. *PLoS Biol.* 3, e159.

Horan, P., Taylor, J., Yamamura, H.I., and Porreca, F. (1992). Extremely long-lasting antagonistic actions of nor-binaltorphimine (nor-BNI) in the mouse tail-flick test. *J. Pharmacol. Exp. Ther.* 260, 1237–1243.

Hoz, L. de, and Simons, M. (2015). The emerging functions of oligodendrocytes in regulating neuronal network behaviour. *BioEssays* 37, 60–69.

Hughes, E.G., Kang, S.H., Fukaya, M., and Bergles, D.E. (2013). Oligodendrocyte progenitors balance growth with self-repulsion to achieve homeostasis in the adult brain. *Nat. Neurosci.* 16, 668–676.

Hughes, E.G., Orthmann-Murphy, J.L., Langseth, A.J., and Bergles, D.E. (2018). Myelin remodeling through experience-dependent oligodendrogenesis in the adult somatosensory cortex. *Nat. Neurosci.* 21, 696–706.

Ibrahim, L.A., Huang, J.J., Wang, S.-Z.Z., Kim, Y.J., Zhang, L.I., and Tao, H.W. (2018). Sparse Labeling and Neural Tracing in Brain Circuits by STARS Strategy: Revealing Morphological Development of Type II Spiral Ganglion Neurons. *Cereb. Cortex* 31, 2759–2772.

Ibrahim, M., Butt, A.M., and Berry, M. (1995). Relationship between myelin sheath diameter and internodal length in axons of the anterior medullary velum of the adult rat. *J. Neurol. Sci.* 133, 119–127.

Jeffries, M.A., Urbanek, K., Torres, L., Wendell, S.G., Rubio, M.E., and Fyffe-Maricich, S.L. (2016). ERK1/2 Activation in Preexisting Oligodendrocytes of Adult Mice Drives New Myelin Synthesis and Enhanced CNS Function. *J. Neurosci.* 36, 9186–9200.

Kessarlis, N., Fogarty, M., Iannarelli, P., Grist, M., Wegner, M., and Richardson, W.D. (2006). Competing waves of oligodendrocytes in the forebrain and postnatal elimination of an embryonic lineage. *Nat. Neurosci.* 9, 173–179.

Kinney, H.C., Brody, B.A., Kloman, A.S., and Gilles, F.H. (1988). Sequence of central nervous system myelination in human infancy. II. Patterns of myelination in autopsied infants. *J. Neuropathol. Exp. Neurol.* 47, 217–234.

Kirby, B.B., Takada, N., Latimer, A.J., Shin, J., Carney, T.J., Kelsh, R.N., and Appel, B. (2006). In vivo time-lapse imaging shows dynamic oligodendrocyte progenitor behavior during zebrafish development. *Nat. Neurosci.* 9, 1506–1511.

Knoll, A.T., and Carlezon, W.A. (2010). Dynorphin, stress, and depression. *Brain Res.* 1314, 56–73.

Koudelka, S., Voas, M.G., Almeida, R.G., Baraban, M., Soetaert, J., Meyer, M.P., Talbot, W.S., and Lyons, D.A. (2016). Individual Neuronal Subtypes Exhibit Diversity in CNS Myelination Mediated by Synaptic Vesicle Release. *Curr. Biol.* 26, 1447–1455.

Krashes, M.J., Shah, B.P., Madara, J.C., Olson, D.P., Strohlic, D.E., Garfield, A.S., Vong, L., Pei, H., Watabe-Uchida, M., Uchida, N., et al. (2014). An excitatory paraventricular nucleus to AgRP neuron circuit that drives hunger. *Nature* 507, 238–242.

Kukley, M., Nishiyama, A., and Dietrich, D. (2010). The fate of synaptic input to NG2 glial cells: neurons specifically downregulate transmitter release onto differentiating oligodendroglial cells. *J. Neurosci.* 30, 8320–8331.

Lacoste, B., Comin, C.H., Ben-Zvi, A., Kaeser, P.S., Xu, X., Costa, L. da F., and Gu, C. (2014). Sensory-Related Neural Activity Regulates the Structure of Vascular Networks in the Cerebral Cortex. *Neuron* 83, 1117–1130.

Larson, V.A., Zhang, Y., and Bergles, D.E. (2016). Electrophysiological properties of NG2+ cells: Matching physiological studies with gene expression profiles. *Brain Res.* 1638, 138–160.

Lee, S., Leach, M.K., Redmond, S.A., Chong, S.Y., Mellon, S.H., Tuck, S.J., Feng, Z.-Q.Q., Corey, J.M., and Chan, J.R. (2012). A culture system to study oligodendrocyte myelination processes using engineered nanofibers. *Nat. Methods* 9, 917–922.

Lin, S., and Bergles, D.E. (2003). Synaptic signaling between GABAergic interneurons and oligodendrocyte precursor cells in the hippocampus. *Nat. Neurosci.* 7, 24–32.

Liu, J., Dietz, K., DeLooyht, J.M., Pedre, X., Kelkar, D., Kaur, J., Vialou, V., Lobo, M., Dietz, D.M., Nestler, E.J., et al. (2012). Impaired adult myelination in the prefrontal cortex of socially isolated mice. *Nat. Neurosci.* 15, 1621–1623.

Liu, J., Dupree, J.L., Gacias, M., Frawley, R., Sikder, T., Naik, P., and Casaccia, P. (2016). Clemastine Enhances Myelination in the Prefrontal Cortex and Rescues Behavioral Changes in Socially Isolated Mice. *J. Neurosci.* 36, 957–962.

Makinodan, M., Rosen, K.M., Ito, S., and Corfas, G. (2012). A Critical Period for Social Experience–Dependent Oligodendrocyte Maturation and Myelination. *Science* 337, 1357–1360.

Maldonado, P.P., and Angulo, M.C.C. (2015). Multiple Modes of Communication between Neurons and Oligodendrocyte Precursor Cells. *Neuroscientist* 21, 266–276.

Marques, S., Zeisel, A., Codeluppi, S., Bruggen, D. van, Falcão, A.M., Xiao, L., Li, H., Häring, M., Hochgerner, H., Romanov, R.A., et al. (2016). Oligodendrocyte heterogeneity in the mouse juvenile and adult central nervous system. *Science* 352, 1326–1329.

Martinez, V.K., Saldana-Morales, F., Sun, J.J., Zhu, P.J., Costa-Mattioli, M., and Ray, R.S. (2019). Off-Target Effects of Clozapine-N-Oxide on the Chemosensory Reflex Are Masked by High Stress Levels. *Front. Physiol.* 10, 521.

Mayoral, S.R., Etxeberria, A., Shen, Y.-A.A., and Chan, J.R. (2018). Initiation of CNS Myelination in the Optic Nerve Is Dependent on Axon Caliber. *Cell Rep.* 25, 544-550.

McKenzie, I.A., Ohayon, D., Li, H., Faria, J.P. de, Emery, B., Tohyama, K., and Richardson, W.D. (2014). Motor skill learning requires active central myelination. *Science* 346, 318–322.

McLaughlin, J., Marton-Popovici, M., and Chavkin, C. (2003). κ opioid receptor antagonism and prodynorphin gene disruption block stress-induced behavioral responses. *J. Neurosci.* 23, 5674–5683.

Mei, F., Mayoral, S.R., Nobuta, H., Wang, F., Despons, C., Lorrain, D.S., Xiao, L., Green, A.J., Rowitch, D., Whistler, J., et al. (2016). Identification of the Kappa-Opioid Receptor as a Therapeutic Target for Oligodendrocyte Remyelination. *J. Neurosci.* 36, 7925–7935.

Mensch, S., Baraban, M., Almeida, R., Czopka, T., Ausborn, J., Manira, A.E., and Lyons, D.A. (2015). Synaptic vesicle release regulates myelin sheath number of individual oligodendrocytes in vivo. *Nat. Neurosci.* 18, 628–630.

Michailov, G.V., Sereda, M.W., Brinkmann, B.G., Fischer, T.M., Haug, B., Birchmeier, C., Role, L., Lai, C., Schwab, M.H., and Nave, K.-A.A. (2004). Axonal neuregulin-1 regulates myelin sheath thickness. *Science* 304, 700–703.

Micheva, K.D., Wolman, D., Mensch, B.D., Pax, E., Buchanan, J., Smith, S.J., and Bock, D.D. (2016). A large fraction of neocortical myelin ensheathes axons of local inhibitory neurons. *eLife* 5, e15784.

Mitew, S., Gobius, I., Fenlon, L.R., McDougall, S.J., Hawkes, D., Xing, Y.L., Bujalka, H., Gundlach, A.L., Richards, L.J., Kilpatrick, T.J., et al. (2018). Pharmacogenetic stimulation

of neuronal activity increases myelination in an axon-specific manner. *Nat. Commun.* 9, 306.

Murphy-Royal, C., Johnston, A.D., Boyce, A.K.J., Diaz-Castro, B., Institoris, A., Peringod, G., Zhang, O., Stout, R.F., Spray, D.C., Thompson, R.J., et al. (2020). Stress gates an astrocytic energy reservoir to impair synaptic plasticity. *Nat. Commun.* 11, 2014.

Murray, J.A., and Blakemore, W.F. (1980). The relationship between internodal length and fibre diameter in the spinal cord of the cat. *J. Neurol. Sci.* 45, 29–41.

Muzumdar, M.D., Tasic, B., Miyamichi, K., Li, L., and Luo, L. (2007). A global double-fluorescent Cre reporter mouse. *Genesis* 45, 593–605.

Osanai, Y., Shimizu, T., Mori, T., Yoshimura, Y., Hatanaka, N., Nambu, A., Kimori, Y., Koyama, S., Kobayashi, K., and Ikenaka, K. (2017). Rabies virus-mediated oligodendrocyte labeling reveals a single oligodendrocyte myelinates axons from distinct brain regions. *Glia* 65, 93–105.

Osso, L.A., and Chan, J.R. (2017). Architecting the myelin landscape. *Curr. Opin. Neurobiol.* 47, 1–7.

Pan, S., Mayoral, S.R., Choi, H.S., Chan, J.R., and Kheirbek, M.A. (2020). Preservation of a remote fear memory requires new myelin formation. *Nat. Neurosci.* 23, 487–499.

Portoghese, P.S., Lipkowski, A.W., and Takemori, A.E. (1987). Binaltorphimine and norbinaltorphimine, potent and selective k-opioid receptor antagonists. *Life Sci.* 40, 1287–1292.

Prigge, J.R., Wiley, J.A., Talago, E.A., Young, E.M., Johns, L.L., Kundert, J.A., Sonsteng, K.M., Halford, W.P., Capecchi, M.R., and Schmidt, E.E. (2013). Nuclear double-fluorescent reporter for in vivo and ex vivo analyses of biological transitions in mouse nuclei. *Mamm. Genome* 24, 389–399.

Redmond, S.A., Mei, F., Eshed-Eisenbach, Y., Osso, L.A., Leshkowitz, D., Shen, Y.-A.A., Kay, J.N., Aurrand-Lions, M., Lyons, D.A., Peles, E., et al. (2016). Somatodendritic Expression of JAM2 Inhibits Oligodendrocyte Myelination. *Neuron* 91, 824–836.

Rishal, I., Kam, N., Perry, R.B., Shinder, V., Fisher, E.M., Schiavo, G., and Fainzilber, M. (2012). A motor-driven mechanism for cell-length sensing. *Cell Rep.* 1, 608–616.

Rosenberg, S.S., Kelland, E.E., Tokar, E., Torre, A.R.D. la, and Chan, J.R. (2008). The geometric and spatial constraints of the microenvironment induce oligodendrocyte differentiation. *Proc. Natl. Acad. Sci. U. S. A.* 105, 14662–14667.

Schindler, A.G., Messinger, D.I., Smith, J.S., Shankar, H., Gustin, R.M., Schattauer, S.S., Lemos, J.C., Chavkin, N.W., Hagan, C.E., Neumaier, J.F., et al. (2012). Stress produces aversion and potentiates cocaine reward by releasing endogenous dynorphins in the ventral striatum to locally stimulate serotonin reuptake. *J. Neurosci.* 32, 17582–17596.

Schüller, U., Heine, V.M., Mao, J., Kho, A.T., Dillon, A.K., Han, Y.-G., Huillard, E., Sun, T., Ligon, A.H., Qian, Y., et al. (2008). Acquisition of Granule Neuron Precursor Identity Is a Critical Determinant of Progenitor Cell Competence to Form Shh-Induced Medulloblastoma. *Cancer Cell* 14, 123–134.

Schwarzer, C. (2009). 30 years of dynorphins--new insights on their functions in neuropsychiatric diseases. *Pharmacol. Ther.* 123, 353–370.

Sharifi, N., Diehl, N., Yaswen, L., Brennan, M.B., and Hochgeschwender, U. (2001). Generation of dynorphin knockout mice. *Mol. Brain Res.* 86, 70–75.

Sharma, K., Schmitt, S., Bergner, C.G., Tyanova, S., Kannaiyan, N., Manrique-Hoyos, N., Kongi, K., Cantuti, L., Hanisch, U.-K.K., Philips, M.-A.A., et al. (2015). Cell type- and brain region-resolved mouse brain proteome. *Nat. Neurosci.* 18, 1819–1831.

Simmons, M.L., Terman, G.W., Gibbs, S.M., and Chavkin, C. (1995). L-type calcium channels mediate dynorphin neuropeptide release from dendrites but not axons of hippocampal granule cells. *Neuron* 14, 1265–1272.

Sohn, J., Hioki, H., Okamoto, S., and Kaneko, T. (2014). Preprodynorphin-expressing neurons constitute a large subgroup of somatostatin-expressing GABAergic interneurons in the mouse neocortex. *J. Comp. Neurol.* 522, 1506–1526.

Steadman, P.E., Xia, F., Ahmed, M., Mocle, A.J., Penning, A.R.A., Geraghty, A.C., Steenland, H.W., Monje, M., Josselyn, S.A., and Frankland, P.W. (2020). Disruption of Oligodendrogenesis Impairs Memory Consolidation in Adult Mice. *Neuron* 105, 1–15.

Stedehouder, J., Brizee, D., Slotman, J.A., Pascual-Garcia, M., Leyrer, M.L., Bouwen, B.L., Dirven, C.M., Gao, Z., Berson, D.M., Houtsmuller, A.B., et al. (2019). Local axonal morphology guides the topography of interneuron myelination in mouse and human neocortex. *eLife* 8, e48615.

Stedehouder, J., Couey, J.J., Brizee, D., Hosseini, B., Slotman, J.A., Dirven, C.M.F.M., Shpak, G., Houtsmuller, A.B., and Kushner, S.A. (2017). Fast-spiking Parvalbumin Interneurons are Frequently Myelinated in the Cerebral Cortex of Mice and Humans. *Cereb. Cortex* 27, 5001–5013.

Sturrock, R.R. (1980). Myelination of the mouse corpus callosum. *Neuropathol. Appl. Neurobiol.* 6, 415–420.

Swire, M., Kotelevtsev, Y., Webb, D.J., Lyons, D.A., and Ffrench-Constant, C. (2019). Endothelin signalling mediates experience-dependent myelination in the CNS. *eLife* 8, e49493.

Takeuchi, T., Duszkiewicz, A.J., and Morris, R.G.M. (2014). The synaptic plasticity and memory hypothesis: encoding, storage and persistence. *Philos. Trans. R. Soc. Lond., B, Biol. Sci.* 369, 20130288.

Taveggia, C., Thaker, P., Petrylak, A., Caporaso, G.L., Toews, A., Falls, D.L., Einheber, S., and Salzer, J.L. (2008). Type III neuregulin-1 promotes oligodendrocyte myelination. *Glia* 56, 284–293.

Taveggia, C., Zanazzi, G., Petrylak, A., Yano, H., Rosenbluth, J., Einheber, S., Xu, X., Esper, R.M., Loeb, J.A., Shrager, P., et al. (2005). Neuregulin-1 type III determines the ensheathment fate of axons. *Neuron* 47, 681–694.

Terman, G., Wagner, J., and Chavkin, C. (1994). Kappa Opioids Inhibit Induction of Long-Term Potentiation in the Dentate Gyrus of the Guinea Pig Hippocampus. *J. Neurosci.* 14, 4740–4747.

Tomassy, G., Berger, D.R., Chen, H.-H., Kasthuri, N., Hayworth, K.J., Vercelli, A., Seung, S.H., Lichtman, J.W., and Arlotta, P. (2014). Distinct Profiles of Myelin Distribution Along Single Axons of Pyramidal Neurons in the Neocortex. *Science* 344, 319–324.

Trapp, B.D., Nishiyama, A., Cheng, D., and Macklin, W. (1997). Differentiation and death of premyelinating oligodendrocytes in developing rodent brain. *J. Cell Biol.* 137, 459–468.

Tremblay, R., Lee, S., and Rudy, B. (2016). GABAergic Interneurons in the Neocortex: From Cellular Properties to Circuits. *Neuron* 91, 260–292.

Viganò, F., Möbius, W., Götz, M., and Dimou, L. (2013). Transplantation reveals regional differences in oligodendrocyte differentiation in the adult brain. *Nat. Neurosci.* 16, 1370–1372.

Voyvodic, J.T. (1989). Target size regulates calibre and myelination of sympathetic axons. *Nature* 342, 430–433.

Wang, F., Ren, S.-Y., Chen, J.-F., Liu, K., Li, R.-X., Li, Z.-F., Hu, B., Niu, J.-Q., Xiao, L., Chan, J.R., et al. (2020). Myelin degeneration and diminished myelin renewal contribute to age-related deficits in memory. *Nat. Neurosci.* 23, 481–486.

Wang, S., Sdrulla, A.D., diSibio, G., Bush, G., Nofziger, D., Hicks, C., Weinmaster, G., and Barres, B.A. (1998). Notch receptor activation inhibits oligodendrocyte differentiation. *Neuron* 21, 63–75.

Whiteus, C., Freitas, C., and Grutzendler, J. (2014). Perturbed neural activity disrupts cerebral angiogenesis during a postnatal critical period. *Nature* 505, 407–411.

Xiao, L., Ohayon, D., McKenzie, I.A., Sinclair-Wilson, A., Wright, J.L., Fudge, A.D., Emery, B., Li, H., and Richardson, W.D. (2016). Rapid production of new oligodendrocytes is required in the earliest stages of motor-skill learning. *Nat. Neurosci.* 19, 1210–1217.

Xin, W., and Chan, J.R. (2020). Myelin plasticity: sculpting circuits in learning and memory. *Nat. Rev. Neurosci.* 21, 682–694.

Yakovleva, T., Bazov, I., Cebers, G., Marinova, Z., Hara, Y., Ahmed, A., Vlaskovska, M., Johansson, B., Hochgeschwender, U., Singh, I.N., et al. (2006). Prodynorphin storage and processing in axon terminals and dendrites. *FASEB J.* 20, 2124–2126.

Yang, S.M., Michel, K., Jokhi, V., Nedivi, E., and Arlotta, P. (2020). Neuron class-specific responses govern adaptive myelin remodeling in the neocortex. *Science* 370, eabd2109.

Yeung, M.S., Zdunek, S., Bergmann, O., Bernard, S., Salehpour, M., Alkass, K., Perl, S., Tisdale, J., Possnert, G., Brundin, L., et al. (2014). Dynamics of oligodendrocyte generation and myelination in the human brain. *Cell* 159, 766–774.

Young, K.M., Psachoulia, K., Tripathi, R.B., Dunn, S.-J.J., Cossell, L., Attwell, D., Tohyama, K., and Richardson, W.D. (2013). Oligodendrocyte dynamics in the healthy adult CNS: evidence for myelin remodeling. *Neuron* 77, 873–885.

Zhang, Y., Chen, K., Sloan, S.A., Bennett, M.L., Scholze, A.R., O’Keeffe, S., Phatnani, H.P., Guarnieri, P., Caneda, C., Ruderisch, N., et al. (2014). An RNA-Sequencing Transcriptome and Splicing Database of Glia, Neurons, and Vascular Cells of the Cerebral Cortex. *J. Neurosci.* 34, 11929–11947.

Zhu, X., Hill, R.A., Dietrich, D., Komitova, M., Suzuki, R., and Nishiyama, A. (2011). Age-dependent fate and lineage restriction of single NG2 cells. *Development* 138, 745–753.

Publishing Agreement

It is the policy of the University to encourage open access and broad distribution of all theses, dissertations, and manuscripts. The Graduate Division will facilitate the distribution of UCSF theses, dissertations, and manuscripts to the UCSF Library for open access and distribution. UCSF will make such theses, dissertations, and manuscripts accessible to the public and will take reasonable steps to preserve these works in perpetuity.

I hereby grant the non-exclusive, perpetual right to The Regents of the University of California to reproduce, publicly display, distribute, preserve, and publish copies of my thesis, dissertation, or manuscript in any form or media, now existing or later derived, including access online for teaching, research, and public service purposes.



Author Signature

6/4/2021

Date